New Serotonin 5-HT$_{2A}$, 5-HT$_{2B}$, and 5-HT$_{2C}$ Receptor Antagonists: Synthesis, Pharmacology, 3D-QSAR, and Molecular Modeling of (Aminoalkyl)benzo and Heterocycloalkanones

José Brea,[†] Jordi Rodrigo,[‡] Antonio Carrieri,[§] Ferran Sanz,[‡] M. Isabel Cadavid,[†] María J. Enguix,[†] María Villazón,[†] Guadalupe Mengod,[‖] Yolanda Caro,[⊥] Christian F. Masaguer,[⊥] Enrique Raviña,[⊥] Nuria B. Centeno,[‡] Angelo Carotti,[§] and M. Isabel Loza*,[†]

Departamento de Farmacología, Facultad de Farmacia, Universidad de Santiago de Compostela, E-15782, Santiago de Compostela, Spain, Research Group on Biomedical Informatics, IMIM, Universitat Pompeu Fabra, C/Drive Aiguader 80, E-08003, Barcelona, Spain, Dipartimento Farmacochimico, University of Bari, Via Orabona, 4, I-70126, Bari, Italy, Departamento de Neuroquímica, Instituto de Investigaciones Biomédicas de Barcelona, CSIC-IDIBAPS, C/Rosselló, 161 Bis, E-08036, Barcelona, Spain, and Departamento de Química Orgánica, Laboratorio de Química Farmacéutica, Facultad de Farmacia, Universidad de Santiago de Compostela, E-15782, Santiago de Compostela, Spain

A series of 52 conformationally constrained butyrophenones have been synthesized and pharmacologically tested as antagonists at 5-HT$_{2A}$, 5-HT$_{2B}$, and 5-HT$_{2C}$ serotonin receptors, useful for dissecting the role of each 5-HT$_2$ subtype in pathophysiology. These compounds were also a consistent set for the identification of structural features relevant to receptor recognition and subtype discrimination. Six compounds were found highly active (pK_i > 8.76) and selective at the 5-HT$_{2A}$ receptor vs 5-HT$_{2B}$ and/or 5-HT$_{2C}$ receptors. Piperidine fragments confer high affinity at the 5-HT$_{2A}$ receptor subtype, with benzofuranone- and thiotetralonepiperidine as the most selective derivatives over 5-HT$_{2C}$ and 5-HT$_{2B}$ receptors, respectively; $K_{i\ 2A/2C}$ and/or $K_{B\ 2A/2B}$ ratios greater than 100 were obtained. Compounds showing a more pronounced selectivity at 5-HT$_{2A}$/5-HT$_{2C}$ than at 5-HT$_{2A}$/5-HT$_{2B}$ bear 6-fluorobenzisoxazolyl- and *p*-fluorobenzoylpiperidine moieties containing one methylene bridging the basic piperidine to the alkanone moiety. An ethylene bridge between the alkanone and the amino moieties led to ligands with higher affinities for the 5-HT$_{2B}$ receptor. Significant selectivity at the 5-HT$_{2B}$ receptor vs 5-HT$_{2C}$ was observed with 1-1[(1-oxo-1,2,3,4-tetrahydro-3-naphthyl)methyl]-4-[3-(*p*-fluorobenzoyl)propyl]piperazine (more than 100-fold higher). Although piperidine fragments also confer higher affinity at 5-HT$_{2C}$ receptors, only piperazine-containing ligands were selective over 5-HT$_{2A}$. Moderate selectivity was observed at 5-HT$_{2C}$ vs 5-HT$_{2B}$ (10-fold) with some compounds bearing a 4-[3-(6-fluorobenzisoxazolyl)]piperidine moiety in its structure. Molecular determinants for antagonists acting at 5-HT$_{2A}$ receptors were identified by 3D-QSAR (GRID-GOLPE) studies. Docking simulations at 5-HT$_{2A}$ and 5-HT$_{2C}$ receptors suggest a binding site for the studied type of antagonists (between transmembrane helices 2, 3, and 7) different to that of the natural agonist serotonin (between 3, 5, and 6).

Introduction

Serotonin (5-HT), a major neurotransmitter found in the central nervous system (CNS), is also present in many peripheral tissues.[1−3] Its numerous biological functions are mediated by a variety of serotonin receptors.[3,4] The interaction with these different serotonin receptors constitutes the mechanism of action of many drugs. In particular, type 2 serotonin receptors (5-HT$_2$) mediate the actions of several drugs used in treating diseases such as schizophrenia, feeding disorders, perception, depression, migraines (prophylactically), hypertension, anxiety, hallucinations, and gastrointestinal dysfunctions.[5,6]

Three 5-HT$_2$ receptor subtypes (5-HT$_{2A}$, 5-HT$_{2B}$, and 5-HT$_{2C}$) show considerable homology at genetic, structural, and functional levels.[3,6,7] All are G-protein coupled receptors (GPCRs) and have been initially associated with activation of phospholipase C via G$_q$-protein. In addition, a variety of other G-protein coupling and effector mechanisms has been described for 5-HT$_2$ receptor subtypes: 5-HT$_{2A}$ receptors can activate phospholipase A$_2$ via G$_{11}$-protein,[8] and they can also mediate decreased cGMP levels, enhancing neurotransmitter release from glutamate terminals;[9] 5-HT$_{2B}$ can bind G$_{11}$[10,11] and increase nitric oxide synthase activity via PDZ-dependent activation;[12] 5-HT$_{2C}$ receptors can mediate increased cGMP levels, when coupled to G$_o$ and/or G$_{11}$ via phospholipase A$_2$.[13]

5-HT$_{2A}$ receptors have been found at high density in the cerebral cortex,[14] mostly in pyramidal cells, and also in interneuronal regions.[14−16] They are also present, at lower density, in the hippocampus, striatum, and other cerebral regions,[14,15] in platelets, and in vascular and uterine smooth muscles.[3,7,17,18]

* To whom correspondence should be addressed. Tel: +34-981-547-139. Fax: +34-981-594-595. E-mail: ffmabel@usc.es.
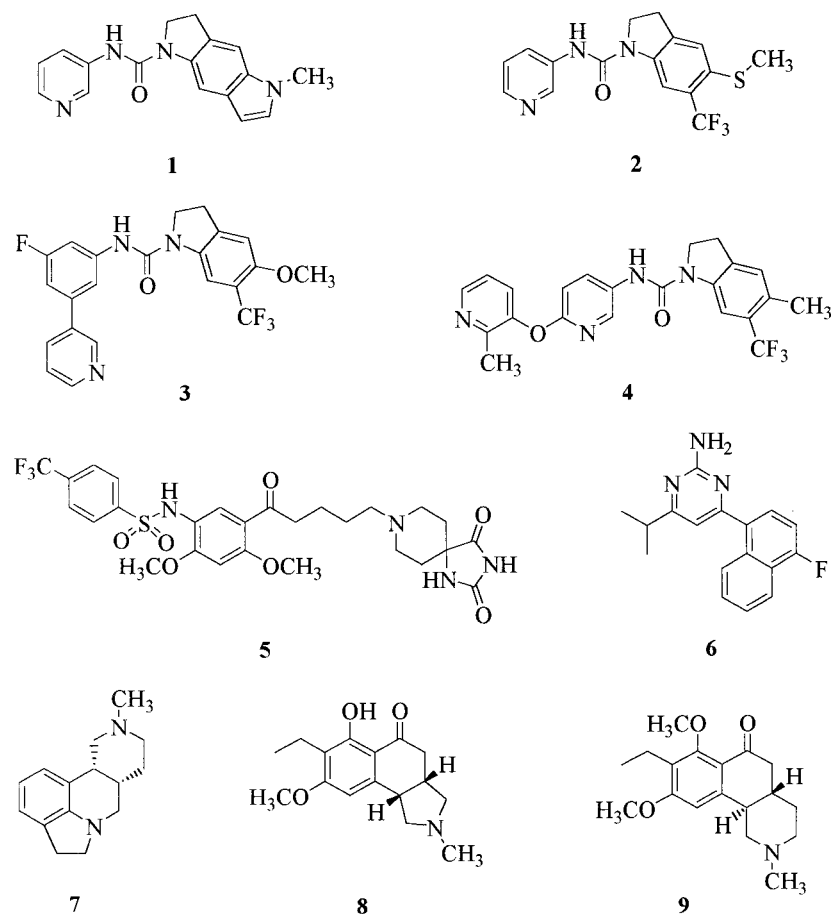† Departamento de Farmacología, Universidad de Santiago de Compostela.
‡ Research Group on Biomedical Informatics, Universitat Pompeu Fabra.
§ Dipartimento Farmacochimico, University of Bari.
‖ Departamento de Neuroquímica, Instituto de Investigaciones Biomédicas de Barcelona.
⊥ Departamento de Química Orgánica, Universidad de Santiago de Compostela.

Chart 1

5-HT$_{2C}$ receptors, first described by Pazos et al.[19] in the choroid plexus, are distributed with varying density in several areas of the brain, including the cortex, basal ganglia, hippocampus, and hypothalamus.[20,21] They have not been found in peripheral tissues.

5-HT$_{2B}$ receptors were originally described as 5-HT$_{1-like}$[22] and 5-HT$_{2F}$[23] and were found to be operationally and functionally similar to 5-HT$_{2A}$ and 5-HT$_{2C}$. Subsequent studies showed that in contrast with 5-HT$_{2A}$, 5-HT$_{2B}$ is blocked only weakly by ketanserin, and operational and structural differences with the 5-HT$_{2C}$ subtype have been described.[3,24] Cloning[23,25] allowed their confident classification as a new subtype of 5-HT$_2$ receptors, 5-HT$_{2B}$.[26] 5-HT$_{2B}$ mRNA is widely distributed in peripheral tissues, having been found in heart, skeletal, and vascular muscles, adipose tissue, the intestine, ovary, uterus, testis, liver, kidney, lung, pancreas, trachea, spleen, thymus, thyroid, and in prostate and salivary glands of mammals.[6,18,27-29] In the CNS, they have been found in the retina and spinal cord and at lower levels in a variety of brain areas.[6,29] Immunochemical studies also suggested their presence in the CNS,[30] although their real presence, distribution, and functions in the brain are still controversial.

Clozapine and other "atypical antipsychotics" have been shown to be effective against the negative symptoms of schizophrenia. The blockade of 5-HT$_2$ receptors has been pointed to as the origin of the distinctive pharmacological profile of these drugs, causing an incidence of tardive diskinaesia and other extrapyramidal side effects that are lower than those found with classical antipsychotics.[31] Clozapine, as well as other atypical antipsychotics, binds not only to 5-HT$_2$ receptors (5-HT$_{2A}$, 5-HT$_{2B}$, and 5-HT$_{2C}$)[32,33] but also, to a different extent, to a number of other GPCRs, including 5-HT$_{1A}$, 5-HT$_6$, 5-HT$_7$, D$_1$, D$_2$, D$_4$, H$_1$, α_1, α_2, M$_1$, M$_2$, and M$_4$.[2,34-41] Despite this lack of specificity, the involvement of 5-HT$_2$ receptors in the pharmacological profile of atypical antipsychotics is supported by many biological, pharmacological, and clinical studies.[42,43] Initially, the 5-HT$_2$ subtype indicated as relevant in schizophrenia by most studies has been 5-HT$_{2A}$.[44-51] However, now it seems possible that some of the effects of atypical antipsychotics that have been attributed to their blocking of 5-HT$_{2A}$ may instead be due to the blockade of 5-HT$_{2B}$ and/or 5-HT$_{2C}$. In particular, affinity for 5-HT$_{2C}$ is an important feature in discriminating classical from atypical antipsychotics.[52] Clozapine, olanzapine, seroquel, and other atypical antipsychotics have indeed greater affinity for 5-HT$_{2C}$ (and in addition for 5-HT$_{2A}$) than for D$_2$ receptors.[53] The blockade of 5-HT$_{2C}$ has been indicated as responsible for relatively mild extrapyramidal side effects observed for atypical antipsychotics, because 5-HT$_{2C}$ rather than 5-HT$_{2A}$ blockade, can prevent the extrapyramidal side effects induced by haloperidol.[54] On the other hand, 5-HT$_{2C}$ antagonists, by enhancing dopamine release in the cortex, would efficiently counteract the hypofrontality that contributes to the deficit symptoms of schizophrenia.[55,56]

A deeper understanding of the roles of 5-HT$_{2A}$, 5-HT$_{2B}$, and 5-HT$_{2C}$ receptors in schizophrenia and in the pharmacology of antipsychotics, as in other CNS and

Table 1. Structures and Codes of Studied Compounds

Cycloalkanone fragments	Amino fragments							
	a	**b**	**c**	**d**	**e**	**f**	**g**	**h**
(indanone-CH₂NRR)	10a[64]		10c		10e[64]		10g[64]	
(tetralone-CH₂NRR)	11a[76]				11e[76]		11g[76]	11h
(indanone-CH₂NRR)	12a				12e[80]		12g[77]	
(F-indanone-CH₂NRR)					13e[80]		13g[77]	
(tetralone-CH₂NRR)	14a[79]				14e[80]		14g[77]	
(benzosuberone-CH₂NRR)							15g[77]	
(indole-ketone-CH₂NRR)	16a[82]				16e[82]		16g[82]	16h[82]
(indole-ketone-CH₂NRR)	17a[82]							
(thieno-ketone-CH₂NRR)	18a[64]		18c		18e[64]		18g[64]	18h[64]
(thieno-ketone-CH₂NRR)					19e[64]		19g[64]	19h[64]
(thieno-ketone-CH₂NRR)	20a[64]		20c		20e[64]		20g[64]	20h[64]
(thieno-ketone-CH₂NRR)							21g[64]	21h[64]
(furano-ketone-CH₂NRR)	22a[84]	22b[84]	22c[84]	22d[84]	22e[84]	22f[84]	22g[84]	22h[84]
(furano-ketone-CH₂NRR)	23a		23c				23g	23h
(carbazolone-CH₂NRR)	24a[81]						24g[81]	24h[81]

peripheral disorders (anxiety, depression, hypertension, etc.), has been hampered by a scarcity of truly selective ligands able to distinguish sharply among these receptor subtypes, especially as regards to differentiation between 5-HT$_{2B}$ and 5-HT$_{2C}$ receptors.

The comparative physiological and pharmacological behaviors of 5-HT$_2$ receptors depend on their structural features. All of the GPCRs share a transmembrane bundle of seven α-helices[57] that in the case of the serotonin and other aminergic receptors, includes the binding site.[58] Structural information on a single GPCR, bovine rhodopsin, is now available. This information was first obtained at low resolution[59] and recently at higher resolution.[57] On the basis of the rhodopsin structural information[57,59] and of additional data coming from molecular biology experiments,[60–63] increasingly accurate models of GPCRs are being produced.[60,61,63–65] These models can be useful for understanding ligand binding and receptor activation features.

Among the reported selective ligands,[66] besides ketanserin, spiperone, MDL100907, and other 5-HT$_{2A}$ selective ligands, some 5-HT$_{2B}$/5-HT$_{2C}$ selective ligands have also been described. A selection of them and their pK_i values at 5-HT$_{2A}$/5-HT$_{2B}$/5-HT$_{2C}$ receptors (in pa-

rentheses) are (Chart 1), pyridylcarbamoylindolines SB-206553 (**1**) (6.3/8.5(pA_2)/8.3)[67] and SB-221284 (**2**) (6.4/7.9/8.6);[68] bisarylcarbamoylindolines SB-228357 (**3**) (6.9/8.0/9.0) and SB243213 (**4**) (6.8/7.0/9.0);[69] benzenesulfonamido-substituted valerophenone RS-102221 (**5**) (6.2/6.5/8.7);[70] naphthylpyrimidine RS-127445 (**6**) (6.3/9.5/6.4);[71] indolonaphthyridine SDZ SER-082 (**7**) (6.2/7.3/7.8);[72] benzo[*e*]isoindolone and benzo[*h*]isoquinolinone derivatives **8** and **9**, respectively, both with a pK_i = 8.0 at the 5-HT$_{2C}$ receptor;[73] and other types of compounds.[74,75]

The chemical heterogeneity of the aforementioned selective ligands, their different affinities for other GPCRs, and their different pharmacokinetic profile prevent an unequivocal attribution of their biological effects at the CNS (especially those related with an antipsychotic profile) to a likely selective interaction with a certain 5-HT$_2$ receptor subtype.

In previous papers,[64,76−84] we have reported different compounds potentially useful to study the structural and pharmacological features of the three 5-HT$_2$ receptor subtypes within a single chemical family, those of the butyrophenones.

The present paper reports the study of a great number of butyrophenones with a large molecular diversity in their alkanone and/or amino moieties (Table 1). To properly explore structure−activity relationships (SAR) and structure−selectivity relationships (SSR), typical N^1-aryl (heteroaryl) substituents, as well as the longer N^1-*p*-fluorobenzoylpropyl and *p*-fluorobenzoyl-butyl substituents, were chosen for the piperazine moiety, whereas N-substitution at the piperidine ring was limited to the benzoyl, *p*-fluorobenzoyl, and 6-fluorobenzisoxazol-3-yl substituents.

In particular, the synthesis and pharmacological profile of the novel butyrophenones are reported here along with new pharmacological data obtained for compounds previously reported by us. Moreover, three-dimensional 3D-QSAR (GRID/GOLPE) models obtained from the study of structural and biological data of the extended set of compounds as well as molecular models arising from docking simulations of selected ligands on 5-HT$_{2A}$ and 5-HT$_{2C}$ receptors are presented and discussed in this paper.

Results and Discussion

A large series of conformationally constrained butyrophenones have been synthesized and pharmacologically tested as antagonists of the 5-HT$_{2A}$, 5-HT$_{2B}$, and 5-HT$_{2C}$ serotonin receptors as useful tools for dissecting the pathophysiological role of each 5-HT$_2$ subtype and for identifying structural features relevant to receptor recognition and subtype discrimination. A partial study of a limited number (28) of these compounds was reported in our preceding paper, which included the determination of 5-HT$_{2A}$ and 5-HT$_{2C}$ activities for 28 and 17 compounds, respectively.[64] Now, the set of compounds has been enlarged by studying 24 new compounds. The pharmacological activities (affinity and antagonistic activity) of the resulting 52 compounds were determined for both 5-HT$_{2A}$ and 5-HT$_{2C}$ receptors. Moreover, the affinity at the 5-HT$_{2B}$ receptor was measured for 43 ligands. The whole set of compounds studied is reported in Table 1, and their affinities are

Scheme 1^a

25

10c
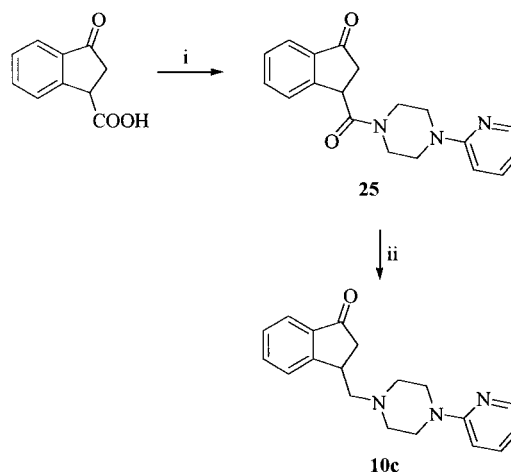
^{a} Reagents: (i) *N*-(2-Pyridyl)piperazine, DCC/HOBt. (ii) (1) (CH$_2$OH)$_2$/*p*-TsOH, (2) LiAlH$_4$, (3) HCl.

Scheme 2^a

11h
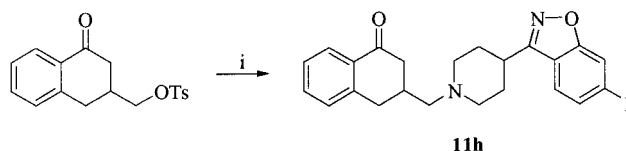
^{a} Reagents: (i) 4-(6-Fluorobenzisoxazol-3-yl)piperidine, NMP.

presented in Table 2. All of the compounds of the series have been designed on the basis of the union of two fragments that share an amino group (see Table 1). The amino moieties **a**, **b**, **c**, and **d** were selected in order to explore slight electronic variations in the phenyl-piperazine structure. Structures **e** and **f** were considered to evaluate the elongation of the corresponding ketanserin moiety (**g**), with the additional difference of considering piperazine instead of piperidine; **g** and **h** were considered because they were the corresponding fragments of ketanserin and risperidone, respectively.

The preparation of compound **10c** was carried out following the same synthetic strategy reported for compounds **10a** and **10g** (Scheme 1).[64] The 3-oxo-indane-1-carboxylic acid[64] was condensed with *N*-(2-pyridyl)piperazine in the presence of 1,3-dicyclohexyl-carbodiimide (DCC) and 1-hydroxybenzotriazole (HOBt) to give the corresponding amide **25**. The ketone group of this compound was protected by ethylene glycol and *p*-toluenesulfonic acid (*p*-TsOH), the amide group was reduced to amine with LiAlH$_4$, and the ethylene ketal was cleaved in acidic medium to afford the amine **10c** in 65% yield from 3-oxo-indane-1-carboxylic acid.

Compound **11h** was synthesized (Scheme 2) from 3-(*p*-toluenesulfonyloxymethyl)-1,2,3,4-tetrahydronaphthalen-1-one[85] via nucleophilic displacement of the tosylate with 4-(6-fluorobenzisoxazol-3-yl)piperidine in *N*-methyl-2-pyrrolidone (NMP) and provided, after bulb to bulb distillation of NMP, the target compound **11h** in 70% yield.

Compound **12a** was prepared according to our procedure used in the synthesis of compound **10c** (Scheme 3). By reaction of (1-oxo-2-indanyl)acetic acid[77] with *N*-(*o*-methoxyphenyl)piperazine, the amide **26** was obtained in 85% yield. Ketalization of the carbonyl group with ethylene glycol and *p*-TsOH, reduction of the amide

**Table 2.** Binding and Functional Data of the Studied Ligands at 5-HT$_2$ Receptors

compd	5-HT$_{2A}$ pK$_i$	5-HT$_{2A}$ pA$_2$	5-HT$_{2B}$ pA$_2$	5-HT$_{2C}$ pK$_i$	K$_B$2A/K$_B$2B[a]	K$_i$2A/K$_i$2C[a]
10a	6.05 ± 0.21	6.21 ± 0.1	7.04 ± 0.2	6.44 ± 0.07	0.15	0.41
10c	<5[b]	nd[c]	6.35 ± 0.03	6.07 ± 0.03	nd	0.027
10e	7.34 ± 0.1	7.20 ± 0.2	<5	<5	501	692
10g	7.58 ± 0.14	8.13 ± 0.09	6.66 ± 0.17	5.96 ± 0.07	30	42
11a	6.29 ± 0.60	6.48 ± 0.50	nd	5.55 ± 0.36	nd	5.5
11e	7.75 ± 0.60	7.27 ± 0.70	<5	<5	589	1778
	6.94 ± 0.20[d]			<5[e]		
11g	8.80 ± 0.80	7.86 ± 0.86	7.2 ± 0.30	6.63 ± 0.14	4.6	148
11h	8.57 ± 0.03	nd	nd	6.98 ± 0.10	nd	39
12a	6.71 ± 0.14	6.8 ± 0.6	nd	6.55 ± 0.20	nd	1.5
12e	6.91 ± 0.60	7.30 ± 0.70	7.5 ± 0.25	5.21 ± 0.07	0.63	50
	7.17 ± 0.15[d]			<5[e]		
12g	8.60 ± 0.80	8.12 ± 0.11	6.43 ± 0.23	6.78 ± 0.07	49	66
13e	7.27 ± 0.10	nd	5.14 ± 0.2	5.71 ± 0.32	nd	36
13g	8.42 ± 0.3	8.12 ± 0.75	6.12 ± 0.4	6.08 ± 0.09	100	219
14a	7.39 ± 0.70	6.72 ± 0.06	7.13 ± 0.48	6.63 ± 0.02	0.39	5.8
14e	7.14 ± 0.70	7.35 ± 0.11	6.8 ± 0.20	5.48 ± 0.14	3.6	46
14g	8.11 ± 0.80	7.47 ± 0.51	7.15 ± 0.21	6.65 ± 0.01	2.1	29
15g	7.88 ± 0.70	6.75 ± 0.60	7.40 ± 0.28	6.30 ± 0.05	0.22	38
16a	6.55 ± 0.80	nd	6.9 ± 0.3	5.44 ± 0.03	nd	13
16e	6.04 ± 0.60	nd	nd	6.63 ± 0.05	nd	0.26
16g	8.06 ± 0.01	nd	nd	7.45 ± 0.01	nd	4.1
16h	8.37 ± 0.80	nd	nd	6.42 ± 0.02	nd	89
17a	7.04 ± 0.70	7.50 ± 0.70	nd	6.65 ± 0.04	nd	2.5
18a	5.82 ± 0.06	5.90 ± 0.01	6.78 ± 0.13	6.04 ± 0.06	0.13	0.60
18c	5.75 ± 0.5	6.40 ± 0.05	5.18 ± 0.18	<5	17	18
18e	6.97 ± 0.13	7.79 ± 0.06	5.60 ± 0.7	5.40 ± 0.12	155	37
18g	7.24 ± 0.12	7.82 ± 0.16	6.88 ± 0.35	6.03 ± 0.04	8.7	16
(−)18h	7.93 ± 0.02	nd	nd	6.95 ± 0.10		
(+)18h	7.94 ± 0.05	nd	nd	6.84 ± 0.07		
(±)18h	8.33 ± 0.11	9.13 ± 0.7	6.24 ± 0.3	6.69 ± 0.12	776	44
19e	7.37 ± 0.15	7.63 ± 0.08	<5	<5	1349	741
19g	8.15 ± 0.13	8.92 ± 0.04	7.06 ± 0.13	6.38 ± 0.06	72	59
19h	8.76 ± 0.2	nd	nd	7.06 ± 0.06	nd	50
20a	6.84 ± 0.12	6.95 ± 0.02	7.19 ± 0.16	7.09 ± 0.17	0.58	0.56
20c	6.76 ± 0.11	6.31 ± 0.50	7.01 ± 0.07	5.77 ± 0.10	0.20	9.8
20e	6.54 ± 0.13	6.83 ± 0.2	6.80 ± 0.07	6.40 ± 0.7	1.0	1.4
20g	8.84 ± 0.17	9.02 ± 0.04	6.35 ± 0.13	6.48 ± 0.06	468	229
20h	8.56 ± 0.20	9.87 ± 0.40	6.23 ± 0.29	6.90 ± 0.05	4365	46
21g	7.95 ± 0.09	nd	6.48 ± 0.1	6.45 ± 0.11	nd	31
21h	8.17 ± 0.18	nd	nd	7.16 ± 0.08	nd	10
22a	<5	nd	6.19 ± 0.20	<5	nd	1.0
22b	7.66 ± 0.05	nd	<5	<5	nd	1445
22c	5.08 ± 0.10	nd	5.46 ± 0.03	6.64 ± 0.02	nd	0.028
22d	<5	nd	6.01 ± 0.24	<5	nd	1.0
22e	6.02 ± 0.03	nd	6.36 ± 0.12	<5	nd	33
22f	5.90 ± 0.04	nd	6.23 ± 0.08	<5	nd	25
22g	7.29 ± 0.20	7.28 ± 0.07	6.71 ± 0.57	<5	3.7	616
22h	7.97 ± 0.03	7.95 ± 0.07	6.61 ± 0.38	<5	22	2951
	8.26 ± 0.12[d]			5.40 ± 0.52[e]		
23a	6.72 ± 0.09	6.30 ± 0.12	6.68 ± 0.23	6.24 ± 0.03	0.42	3.0
23c	6.45 ± 0.01	6.17 ± 0.06	<5	<5	47	89
23 g	7.71 ± 0.17	7.58 ± 0.20	6.63 ± 0.19	6.46 ± 0.03	8.9	18
23h	8.97 ± 0.09	9.25 ± 0.05	6.30 ± 0.01	7.16 ± 0.01	891	65
	9.14 ± 0.11[d]			7.46 ± 0.30[e]		
24a	6.20 ± 0.61	6.50 ± 0.20	6.80 ± 0.05	5.92 ± 0.06	0.50	1.9
24g	8.04 ± 0.80	9.20 ± 0.27	7.22 ± 0.23	6.23 ± 0.09	96	65
24h	8.80 ± 0.88	9.50 ± 0.32	6.35 ± 0.10	7.24 ± 0.06	1412	36
	8.93 ± 0.15[d]			7.56 ± 0.26[e]		
haloperidol	7.28 ± 0.03			5.34 ± 0.03		
clozapine	8.12 ± 0.07	9.16	6.77 ± 0.2	7.80 ± 0.1		
ketanserin	8.29 ± 0.04	8.87 ± 0.11		7.36 ± 0.1		
risperidone	9.51 ± 0.03			7.38 ± 0.03		

[a] K_i and K_B ratios. [b] Values <5 were arbitrarily substituted by 4.5 to allow the calculations of K_i and K_B ratios. [c] nd = not determined. [d] Data obtained from human 5-HT$_{2A}$ receptors transfected into CHO cells. [e] Data obtained from human 5-HT$_{2C}$ receptors transfected into HeLa cells.

group with LiAlH$_4$, and subsequent ketone deprotection in acidic medium produced the desired amine **12a**, in 70% yield. The preparation of compound **20c** was carried out following the same route: (4-oxo-4,5,6,7-tetrahydrobenzo[*b*]thiophen-5-yl)acetic acid[64] was condensed with *N*-(2-pyridyl)piperazine in the presence of DCC/HOBt

to give the amide **27**. The ketonic group was protected with ethylene glycol and *p*-TsOH, the amide group was reduced to amine with LiAlH$_4$, and the ethylene ketal was cleaved in acidic medium to afford the amine **20c** in 70% yield from (4-oxo-4,5,6,7-tetrahydrobenzo[*b*]-thiophen-5-yl)acetic acid.

Scheme 3[a]

X = HC=CH, S
n = 0, 1

X = HC=CH, n = 0, **26**
X = S, n = 1, **27**

X = HC=CH, n = 0, **12a**
X = S, n = 1, **20c**
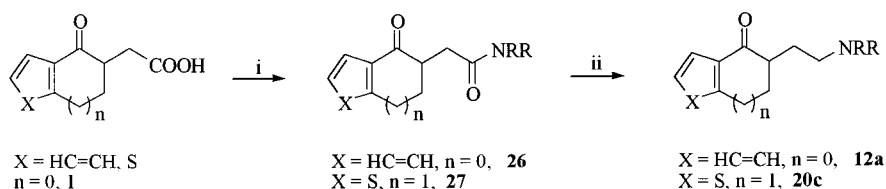
[a] Reagents: (i) N-(2-Pyridyl)piperazine, DCC/HOBt. (ii) (1) $(CH_2OH)_2$/p-TsOH, (2) $LiAlH_4$, (3) HCl.

Scheme 4[a]

28

18c
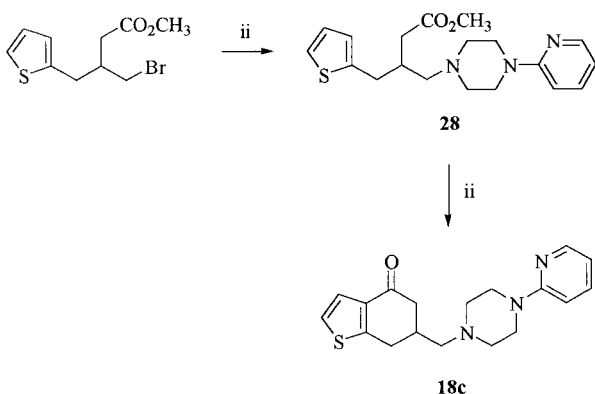
[a] Reagents: (i) N-(2-Pyridyl)piperazine, KI, Na_2CO_3. (ii) PPA.

Scheme 5[a]

29

23a, 23c, 23g, 23h

30-33
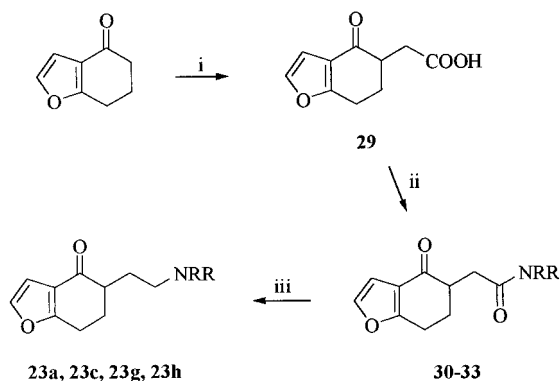
[a] Reagents: (i) (1) $BrCH_2CO_2Et$/LDA, (2) KOH. (ii) HNRR, DCC/HOBt. (iii) (1) $(CH_2OH)_2$/p-TsOH, (2) $LiAlH_4$, (3) HCl.

The preparation of compound **18c** was carried out following the synthetic strategy shown in Scheme 4. Methyl γ-bromo-β-(2-thienyl)butyrate[64] underwent nucleophilic substitution with N-(2-pyridyl)piperazine in basic methyl isobutyl ketone to give the β-aminoester **28** in 95% yield. Finally, acid-catalyzed ring closure with polyphosphoric acid (PPA) afforded compound **18c** in 40% yield.

Compounds **23a**, **23c**, **23g**, and **23h** were prepared by amide-linking the two moieties, protecting nonamide carbonyls as ketals, reducing the amide carbonyl, and deprotecting (Scheme 5). Alkylation of 4,5,6,7-tetrahydrobenzo[b]furan-4-one with lithium diisopropylamide at −70 °C, followed by quenching with ethyl bromoacetate, gave ethyl ester that was then hydrolyzed to the thienocycloalkanone acetic acid **30** in 50% overall yield. The amides **30−33** were prepared in good yields by direct acid−amine coupling, with carboxylate activation by DCC in the presence of HOBt. Ketalization of carbonyl groups with ethylene glycol and p-TsOH or pyridinium tosylate in anhydrous toluene, with azeotropic distillation of water in a Dean−Stark apparatus,
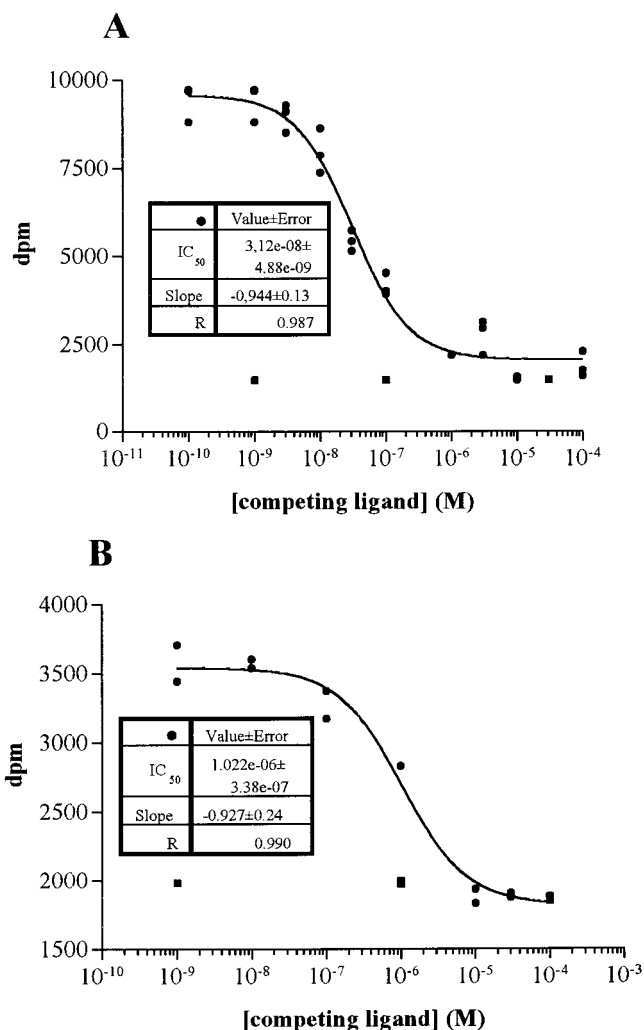
A

B

Figure 1. Binding competition experiments; a representative experiment is shown with compound **24g** at (A) 5-HT_{2A} binding sites in rat frontal cortex, the radioligand used was [³H]-ketanserin (●), nonspecific binding was measured with 10^{-6} M metisergide (■), and the assay was performed with triplicate points and (B) 5-HT_{2C} binding sites in bovine choroid plexus, the radioligand used was [³H]mesulergine (●), nonspecific binding was measured with 10^{-6} M mianserine (■), and the assay was performed with duplicate points. A total of three experiments was carried out in each case.

provided the corresponding ethylene ketals, which were reduced with $LiAlH_4$ without further purification. Finally, deketalization to restore carbonyl groups in acidic medium gave the amines **23a**, **23c**, **23g**, and **23h**.

Figure 1 shows binding competition experiments carried out with [³H]-ketanserin and [³H]-mesulergine in rat cortex and bovine choroids plexus (5-HT_{2A} and 5-HT_{2C}, respectively), for ligand **24g**. All of the active compounds showed competition concentration−response curves of specific radioligand binding against increasing
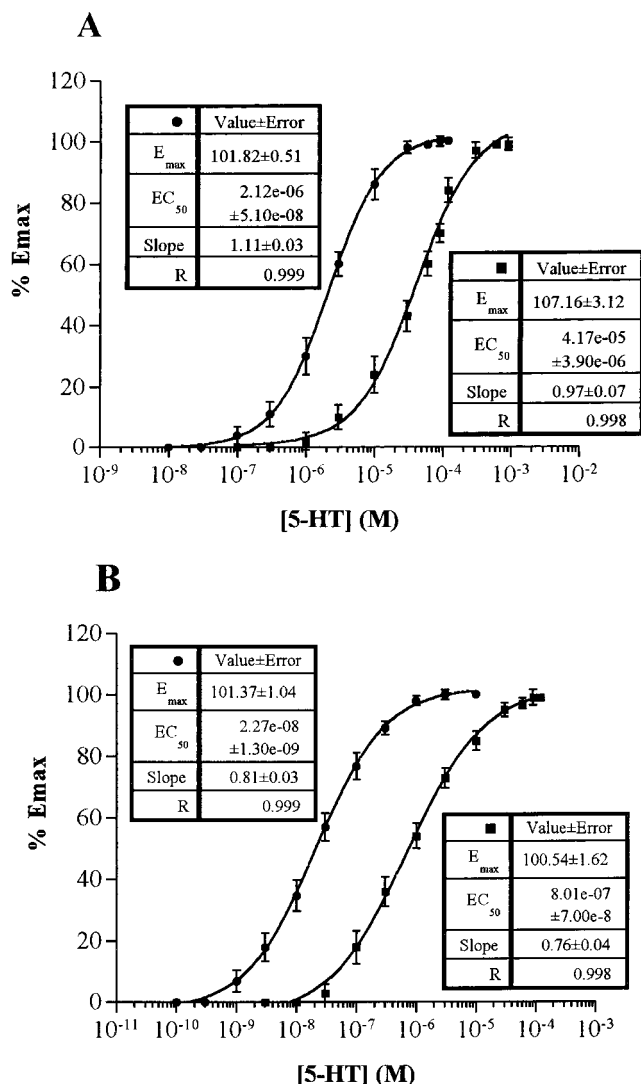
A

B

Figure 2. Functional assays; an example is shown with compound **13g** at (A) 5-HT$_{2A}$ receptors in smooth muscle of rat thoracic aorta, cumulative concentration−response curves to 5-HT in the absence (●) and in the presence (■) of 10^{-7} M **13g** and (B) 5-HT$_{2B}$ receptors in rat stomach fundus, cumulative concentration−response curves to 5-HT in the absence (●) and in the presence (■) of 10^{-5} M **13g**. Points are the mean of four experiments in each case, vertical bars show sem.

concentrations of ligands, the slopes not being significantly different from unity at the 5% level of statistical significance.

Figure 2 shows 5-HT concentration−response curves in rat aorta (5-HT$_{2A}$ receptor) and rat stomach fundus (5-HT$_{2B}$ receptor) for compound **13g**. All of the active compounds concentration dependently displaced these curves to the right in a parallel way without depression of their maximum, which is the typical behavior of competitive antagonists.

The numerous compounds, as well as the good spread of the biological data obtained from the present data set, permit a detailed and robust SAR analysis for the three serotonin 5-HT$_2$ receptors, also at the 3D quantitative level. To avoid the loss of meaningful information from the SSR analysis, affinity values <5 were arbitrarily fixed at 4.50 and these arbitrary values were used to calculate the K_i and K_B ratios reported in Table 2.

Data in Table 2 show widely distributed 5-HT$_{2A}$ pK_i values (4.47 log units, if 4.5 is arbitrarily assigned to values <5, $n = 52$) and less spread 5-HT$_{2C}$ pK_i values (2.95 log units, if 4.5 is assigned to values <5, $n = 52$). The 5-HT$_{2B}$ pA_2 values are also moderately spread (3.00 log units, if again 4.5 is assigned to values <5, $n = 43$).

A preliminary data analysis shows no significant pairwise correlations among the activities at the three receptors subtypes, suggesting different binding modes and/or different binding sites. The antagonist activities toward 5-HT$_{2A}$ expressed as pA_2 were generally even higher than the corresponding binding affinities (pK_i), indicative of an efficient transductor−effector amplification of the signal in functional assays, making these compounds of potential pharmacological interest. There is a good correlation between pK_i and pA_2 data ($r^2 = 0.723$) for the 5-HT$_{2A}$ receptor. This result suggests a notable similarity between binding and functional response in central and peripheral 5-HT$_{2A}$ receptors.

The highest 5-HT$_{2A}$ affinities were observed for cycloalkanones bearing piperidine fragments (19 compounds: **23h**, **20g**, **11g**, **24h**, **19h**, **12g**, **11h**, **20h**, **13g**, **16h**, **18h**, **21h**, **19g**, **14g**, **16g**, **24g**, **22h**, **21g**, and **15g**, all with pK_i > 7.8), with **23h** as the most potent compound (pK_i = 8.97), whereas most of the lowest affinities corresponded to piperazine derivatives (13 compounds: **23c**, **11a**, **24a**, **10a**, **16e**, **22e**, **22f**, **18a**, **18c**, **22c**, **10c**, **22a**, and **22d**, all with pK_i < 6.5).

As far as the binding to 5-HT$_{2C}$ receptor subtype is concerned, highest affinities were generally obtained for piperidine derivatives (**16g**, **24h**, **21h**, **23h**, **20a**, **19h**, **11h**, and **20h**, pK_i ≥ 6.9), with **16g** as the most potent compound (pK_i = 7.45), whereas lowest affinities corresponded to piperazine derivatives (**14e**, **16a**, **18e**, **12e**, **22g**, **22h**, **22e**, **22f**, **22a**, **22d**, **18c**, **11e**, **22b**, **19e**, **10e**, and **23c**, pK_i < 5.5). Ligands carrying the aminomethylbenzofuranone moiety showed pK_i values lower than 5 (**22g**, **22h**, **22e**, **22f**, **22a**, **22d**, and **22b**) with the exception of the 2-pyridyl-4-piperazine derivative **22c** (pK_i = 6.64).

For 5-HT$_{2B}$ receptor ligands, a less clear picture came from the analysis of their pA_2 values, since they represent activities involving indirect measures, and consequently, transducer−effector coupling can induce some interferences, especially when there are no compounds with really high potency. Indeed, the highest and lowest pA_2 values were displayed by compounds **12e** (pA_2 = 7.50) and **11e** (pA_2 = 4.50), respectively, both sharing the same piperazine fragment and having relatively similar cycloalkanone moieties. Another strong and unexpected effect was the dramatic drop in activity, from 7.50 to 5.14, resulting from the introduction of a fluorine atom in the cycloalkanone moiety (**13e**) in comparison with the highest affinity ligand **12e**. Interestingly, eight of the top 10 high affinity ligands bear an aminoethylcycloalkanone moiety, whereas four out of five bottom low affinity ligands present an aminomethyl moiety.

Compounds with high selectivity for the 5-HT$_{2A}$ receptor subtype (vs 5-HT$_{2B}$ and 5-HT$_{2C}$) were obtained: compounds **22h**, **11e**, **22b**, **19e**, **10e**, **22g**, **20g**, **13g**, and **11g** all displayed 5-HT$_{2A}$/5-HT$_{2C}$ K_i ratios higher than 100, the most selective compound being the benzofuranone-piperidine derivative **22h** that shows a

pK_i = 7.97 at the 5-HT$_{2A}$ receptor and a K_i $_{2A/2C}$ ratio of 2951. 5-HT$_{2A}$/5-HT$_{2B}$ selectivity was studied based on antagonistic potency (pA_2), because this was the only pharmacological parameter that was determined for both receptors. Good selectivity (higher than 100) for 5-HT$_{2A}$ over 5-HT$_{2B}$ was found for compounds **20h**, **24h**, **19e**, **23h**, **18h**, **11e**, **10e**, **20g**, **18e**, and **13g**, and the highest selectivity (K_B ratio = 4365) was associated to the thiotetralone-piperidine ligand **20h** that also possesses an outstanding affinity for the 5-HT$_{2A}$ receptor subtype (pA_2 = 9.87). A comparative analysis of the 5-HT$_{2A}$/5-HT$_{2C}$ (K_i) vs 5-HT$_{2A}$/5-HT$_{2B}$ (K_B) activity ratios indicates that compounds **11e**, **19e**, **10e**, **20g**, **13g**, and **12g** exhibit a high selectivity for the 5-HT$_{2A}$ receptor vs both the 5-HT$_{2B}$ and the 5-HT$_{2C}$ receptors. In contrast, three compounds show 5-HT$_{2A}$/5-HT$_{2C}$ selectivities that are more pronounced than those of 5-HT$_{2A}$/5-HT$_{2B}$: **22h** (2951 vs 22), **22g** (616 vs 3.7), and **11g** (148 vs 4.6). These three compounds are 6-fluorobenzisoxazol-3-yl and *p*-fluorobenzoylpiperidine derivatives with one methylene bridging the basic piperidine to the alkanone moiety. These structural features may be useful in designing high affinity 5-HT$_{2A}$ ligands with higher selectivity vs 5-HT$_{2C}$ than 5-HT$_{2B}$. 5-HT$_{2A}$/5-HT$_{2B}$ selectivities greater than 5-HT$_{2A}$/5-HT$_{2C}$ resulted for compounds **20h** (4365 vs 46), **24h** (1412 vs 36), and **23h** (891 vs 65), all bearing 6-fluorobenzisoxazol-3-yl piperidine moieties but linked through different bridges to varying alkanones.

It is worth noting that all of the 5-HT$_{2C}$ selective ligands bear a substituted piperazine as the basic moiety. 5-HT$_{2C}$/5-HT$_{2A}$ selectivity was observed only for very few compounds (**18a**, **20a**, **10a**, **16e**, **22c**, and **10c**), the last two presenting the lowest 5-HT$_{2A}$/5-HT$_{2C}$ K_i ratios (0.028 and 0.027), corresponding to 5-HT$_{2C}$ affinities (37- and 36-fold higher than 5-HT$_{2A}$, respectively). Unfortunately, this selectivity is associated to a relatively low affinity for the 5-HT$_{2C}$ receptor subtype (6.64 and 6.07, respectively). Moderate selectivity for 5-HT$_{2C}$ receptor vs 5-HT$_{2B}$ (10-fold) was observed in some fluorobenzisoxazo-3-yl-piperidine ligands.

Only a few ligands, **20c**, **10a**, and **18a**, elicited a small but significant selectivity for 5-HT$_{2B}$ over 5-HT$_{2A}$ receptor, with 7.6-, 6.7-, and 5.01-fold preference, respectively. All of these ligands showed relatively good affinities and carry a substituted piperazine moiety. Important selectivity at the 5-HT$_{2B}$ receptor over 5-HT$_{2C}$ was observed for compound **12e**, which is a *p*-fluoro-benzoyl-propyl-piperazine derivative.

The salient results emerging from the previous SAR and SSR analyses may be summarized as follows: (i) Compounds containing a piperidine fragment exhibit high affinity for the 5-HT$_{2A}$ receptor, while those having benzofuranone or thiotetralone-piperidine moieties are the most selective derivatives for 5-HT$_{2A}$ in comparison to 5-HT$_{2C}$ and 5-HT$_{2B}$, respectively. (ii) Although the piperidine fragment is associated with higher affinities for the 5HT$_{2C}$ receptors than the piperazine one, only piperazine-containing ligands were selective for 5-HT$_{2C}$ in comparison to 5-HT$_{2A}$. (iii) An ethylene bridge between the alkanone and the amino moieties led to ligands with the highest affinities for the 5-HT$_{2B}$ receptor. (iv) Compounds showing a 5-HT$_{2A}$/5-HT$_{2C}$ selectivity greater than the 5-HT$_{2A}$/5-HT$_{2B}$ one bear 6-fluorobenz-

isoxazol-3-yl or *p*-fluorobenzoyl-piperidine moieties as well as a single methylene bridging the basic piperidine and the alkanone moiety.

To gain more insight into the main interactions underlying selective binding of the studied series of compounds to the three receptor subtypes, also at a quantitative and 3D level, the same data set found in Table 2 was analyzed by means of 3D-QSAR and docking studies. Affinity and activity data (pK_i and pA_2) lower than 5 were not used in the 3D-QSAR studies.

3D-QSAR approaches rely on advanced statistical methods to correlate the dependent variable (usually the biological activity) with 3D chemical descriptors, such as molecular interaction potentials, which are interaction energies of the considered molecules with proper molecular probes. In the past, the majority of such studies have been carried out by means of comparative molecular field analysis (CoMFA) developed by Cramer more than 10 years ago.[86] In the past few years, the so-called GRID/GOLPE[87] approach has also been used as a successful improvement over CoMFA. Although CoMFA and GRID/GOLPE rely on the same principles and similar statistical algorithms, GRID offers an excellent set of molecular probes for the computation of interaction potentials, and GOLPE provides, besides a classical PLS method,[88] different useful tools for data pretreatment, variable selection, and results interpretation. This often leads to more meaningful results and limits the risk of deriving over fitted models.

In our previous study of a subset of the present series of compounds,[64] we performed a CoMFA analysis leading to the identification, at the 3D level, of the main molecular determinants for a high 5-HT$_{2A}$ receptor binding affinity, within the limited considered series. In that study, we found that the steric, lipophilic, and electrostatic properties of the ligands play an essential role in the binding to the 5-HT$_{2A}$ receptor.

We selected the GRID/GOLPE approach for our new 3D-QSAR studies because its aforementioned objective advantages in comparison with the classical CoMFA approach. Indeed, the atom probes available in GRID[89] for the calculation of the molecular interaction fields are much more numerous than those implemented in CoMFA and most of them better resemble the functional groups of amino acids constituting the putative binding site of enzymes and receptors. For the present study, we chose four probes (hydroxyl, C$_{sp^3}$, N$^+_{sp^3}$, DRY), according to the nature of the amino acids forming the antagonist binding site of the 5-HT$_2$ receptors as it is discussed in the docking simulation section. Another advantage of GRID/GOLPE is that it includes advanced mathematical tools such as variable pretreatment, D-Optimal, and FFD variable selection methods as well as smart region definition (SRD).[90] This allows one to obtain more robust and easily interpretable 3D-QSAR models.

The results of the GRID/GOLPE analyses of the three different binding data sets (5-HT$_{2A}$ pK_i, 5-HT$_{2B}$ pA_2, and 5-HT$_{2C}$ pK_i), carried out using the four selected probes, are summarized in Table 3. Models with high statistical coefficients were obtained only in the analysis of the 5-HT$_{2A}$ binding data whereas the analysis of the 5-HT$_{2B}$ and 5-HT$_{2C}$ data yielded poorer models. It is noteworthy that for 5-HT$_{2A}$, the four different probes gave PLS

Table 3. Statistical Results of the GRID/GOLPE Analyses on 5-HT$_{2A-C}$ Ligands

receptor	probe[b]	n^c	var[d]	ONC	$q^{2\,e}$	$r^{2\,f}$
5-HT$_{2A}$	hydroxyl (O1)	49[a]	1695	4	0.815	0.883
	N$^+$ sp^3 (N3+)	49[a]	1696	4	0.828	0.887
	C sp^3 (C3)	49[a]	1536	4	0.830	0.891
	DRY	49[a]	1893	4	0.842	0.932
5-HT$_{2B}$	hydroxyl (O1)	38	2075	3	0.136	0.529
	N$^+$ sp^3 (N3+)	38	2000	3	0.177	0.517
	C sp^3 (C3)	38	1273	1	0.247	0.403
	DRY	38	1637	1	0.371	0.541
5-HT$_{2C}$	hydroxyl (O1)	41	963	1	0.378	0.489
	N$^+$ sp^3 (N3+)	41	1013	1	0.399	0.519
	C sp^3 (C3)	41	1441	1	0.353	0.481
	DRY	41	1983	4	0.341	0.866

[a] Compound **22b** was excluded from the analysis. [b] The letters in parentheses refer to the GRID probe code. [c] n = number of data points. [d] var = number of variables remaining after pretreatment. [e] q^2 = squared cross-validated correlation coefficient. [f] r^2 = squared correlation coefficient.
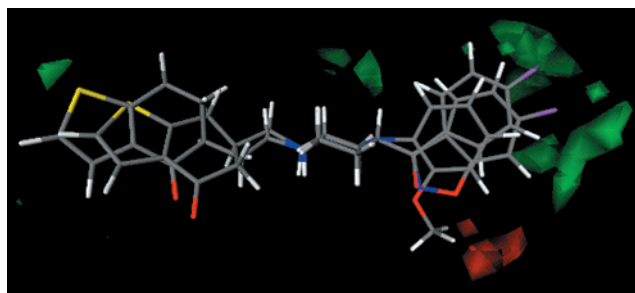
Figure 3. GRID/GOLPE PLS coefficient contour map for 5-HT$_{2A}$ receptor ligands (O1 probe; contour levels: 0.005 green and -0.005 red; for color code, see text). Compounds **20g** (QF0601B), **20h** (QF0610B), and **18a** (QF0607B) are displayed to aid interpretation.

models with similar statistical figures (see Table 3). These findings support the hypothesis that the binding process of our ligands to the 5-HT$_{2A}$ receptor is influenced by a combination of steric, electrostatic, hydrophobic, and hydrogen bonding interactions as assessed by C$_{sp^3}$, N$^+_{sp^3}$, DRY, and hydroxyl probes, respectively.

Moreover, it is rather interesting to observe that the present statistical results are highly comparable with those found in our previous 3D-QSAR study conducted with CoMFA on a reduced set of ligands.[64] The importance of the steric, electrostatic, and lipophilic effects in the modulation of the binding process was clearly highlighted in both studies. As an important complement to previous CoMFA results, GRID/GOLPE allowed us to elucidate the role of hydrogen bonding in the receptor binding of our ligands, by using the hydroxyl probe provided by GRID.

From site-directed mutagenesis studies, it has been postulated that hydroxyl groups of some serine residues present in the third transmembrane α-helix region of the serotoninergic receptor family may form important hydrogen bonds with the ligands.[61] This hypothesis was fully supported by our GRID/GOLPE results. As can be seen from the graphical representations of the PLS coefficients in Figure 3, there are regions around the ligands where the different substituents of our derivatives could generate favorable (green) or unfavorable (red) interactions with the hydroxyl probe. Green polyhedra appear in the region surrounding the fluoro atoms of the highly active compounds **20g** and **20h**, suggesting a possible favorable hydrogen bond interaction for both

derivatives. Red polyhedra represent zones where the receptor poorly tolerates the presence of even small groups, such as the methoxy group of the low activity compound **18a**. On the other hand, a small but significant green polyhedron appears close to the carbonyl oxygen and the sulfur atom of the hetero-fused cycloalkanone moiety of the highly active ligands **20g** and **20h**, indicating a favorable zone for hydrogen bonding or dipole–dipole interaction. The other probes, C$_{sp^3}$, N$^+_{sp^3}$, and DRY, gave PLS coefficient contour maps fully compatible with that previously developed with CoMFA by using steric, electrostatic, and lipophilic (MLP[91] calculations) fields. One strong outlier (compound **22b**) was omitted from the analysis. Its elimination can be justified, at least in part, considering its unique chemical structure; it is the only ligand bearing an unsubstituted phenyl ring attached to the piperazine ring.

The lack of significant PLS models for the 5-HT$_{2B}$ receptor subtype could be partially ascribed to the nature of the biological data, which are functional and not binding experiments. In other words, the functional response is inherently a very complex event, most likely unrelated to the classical physicochemical properties commonly used to describe receptor–ligand interactions. Moreover, the spread and distribution of affinity data for the 5-HT$_{2B}$ receptor subtype were not as good as for 5-HT$_{2A}$. Because of these intrinsic limitations, no further effort was made to improve the statistics of the PLS models for the 5-HT$_{2B}$ receptor subtype shown in Table 3.

Also, in the modeling of 5-HT$_{2C}$ binding affinity, we obtained PLS models with modest fitting and quite unsatisfactory predictive power ($r^2 \leq 0.87$; $q^2 \leq 0.34$) (see Table 3). A possible reason for this lack of predictive power could be ascribed to the small variability of the 5-HT$_{2C}$ data in comparison with that of the 5-HT$_{2A}$. On the other hand, it has to be pointed out that the same ligand alignment was used for all of the GRID/GOLPE analyses (see the Experimental Section). This could be a source of inaccuracy of the models obtained for two of the receptors, since the comparative docking simulations described below show significantly different binding geometries of the two considered ligands in the models of 5-HT$_{2A}$ and 5-HT$_{2C}$ receptors. In any case, poorer statistics were obtained by testing alternative ligand superpositions (data not shown).

To gain insight on the molecular features governing the binding process of the studied series of antagonists, we performed computational simulations of the docking of two of the studied compounds (**20c** and **20h**) into models of the rat 5-HT$_{2A}$ and human 5-HT$_{2C}$ receptors (the species were selected in agreement with the biological data). Compounds **20c** and **20h** were selected because despite having the structural differences concentrated in a single molecular fragment (the amino moiety), they exhibit completely different pharmacological profiles. Thus, while compound **20h** shows one of the highest 5-HT$_{2A}$ affinities (the highest pA_2 in functional assays) and a relatively high 5-HT$_{2C}$ affinity, compound **20c** has a relatively low 5-HT$_{2A}$ affinity and an even worse 5-HT$_{2C}$ one. A second important argument for the selection of compounds **20c** and **20h** was their relatively low number of conformational degrees of freedom.
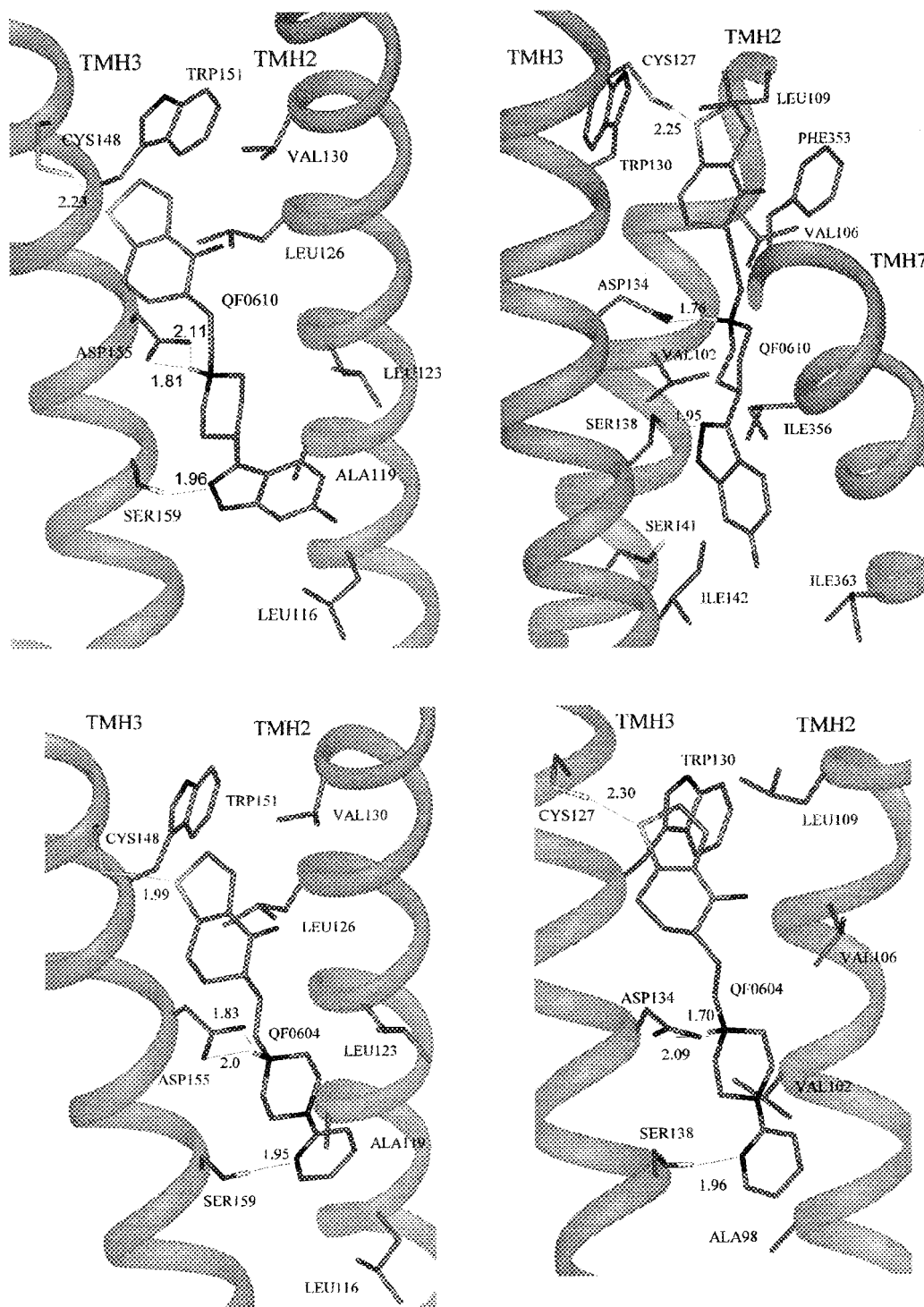
Figure 4. Models of the docking of **20h** (QF0610B) (top) and **20c** (QF0604B) (bottom) into the 5-HT$_{2A}$ (left) and 5-HT$_{2C}$ (right) receptors.

The models of the receptors were built following the protocol indicated in the corresponding experimental section, and they were successfully assessed in different ways: (a) We did not find significant contradictions between our models and the topology of the recently published crystal structure of rhodopsin[57] (for instance, both have the same relative positions of the highly conserved residues, including the network of hydrogen bonds between transmembrane helices 1, 2, and 7 (TMH1, TMH2, and TMH7), which involves the highly conserved Asn of TMH1). (b) A quality assessment performed using the Procheck software[92] resulted in

excellent quality parameters and plots. (c) Molecular dynamics simulations using AMBER 4.1, during 1 ns at 310 K, did not produce any significant distortion in the model. (d) An automatic exploration of the docking of the natural agonist, serotonin, carried out with the QXP program[93] placed this agonist in a pocket between TMH3, TMH5, and TMH6, yielding experimentally known interactions with Asp155[63] and Ser159[61] in both receptors and with Ser239 in 5-HT$_{2A}$ and Ser219 in 5-HT$_{2C}$.[94–96]

The docking of the two antagonists in the models of the two receptors (rat 5-HT$_{2A}$ and human 5-HT$_{2C}$) was
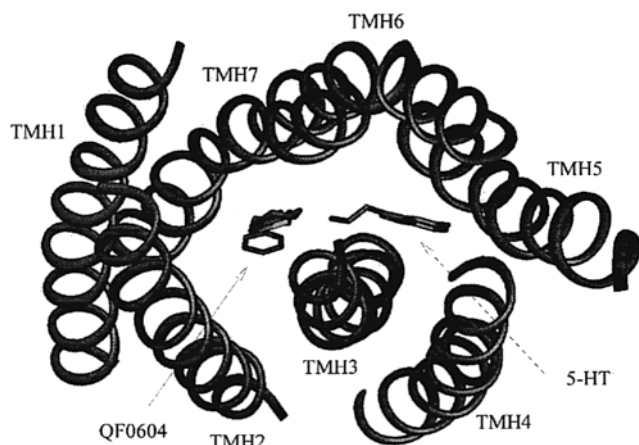
Figure 5. Comparison of the docking positions in the 5-HT$_{2A}$ receptor obtained for an agonist (serotonin) and an antagonist (**20c** (QF0604B)).

automatically explored by means of 300 runs of the MCDOCK module of the QXP program. Figure 4 shows the lowest energy docking complexes (one per molecule and per receptor) found along the docking simulations. It has to be pointed out that in all of the docking complexes obtained, the antagonists were always automatically located between helices TMH2, TMH3, and TMH7, exhibiting an extended conformation approximately parallel to the axes of the helices. Hydrogen bond interactions with three residues in TMH3 (Cys148, Asp155, and Ser159) were obtained in all of the cases. Hydrophobic interactions with residues in TMH2 and TMH7 also stabilized the complexes. The performed docking simulations performed were unable to explain the pK_i differences between the considered ligands and the receptors being considered. This limitation could be caused by imperfections in the models of the receptors or in the QXP docking software. It has to be pointed out that even slight inexactnesses in geometric parameters provoke notable changes in the energy values resulting from molecular modeling computations.

The resulting docking positions of the antagonists studied are totally different from those previously described for the natural agonist 5-HT, and they are similar to those obtained by other authors when simulating the docking of different 5-HT$_{2C}$ antagonists in the corresponding receptor model.[66] It has to be pointed out that even initially placing the antagonists in the binding pocket between TMH3, TMH5, and TMH6, with the amino group of the ligand in front of Asp155 of TMH3, QXP explorations yield docking positions in the pocket between TMH2, TMH3, and TMH7, as those shown in Figure 4. An opposite experiment that consisted in placing an agonist (5-HT) between TMH2, TMH3, and TMH7 and carrying out a QXP exploration yielded the above-described docking position of serotonin between TMH3, TMH5, and TMH6. Figure 5 illustrates the different binding positions of an agonist (5-HT) and an antagonist (**20c**) obtained when simulating their docking into the 5-HT$_{2A}$ receptor. There are experimental indications (mutations of the serines in TMH5) that antagonists structurally related to the present series (i.e., ketanserin) do not directly interact with TMH5.[61,94] On the other hand, the packing of the extracellular loops described in the recent experimental structure of rhodopsin[57] shows two entrances into the transmembrane

bundle in agreement with the two aforementioned binding positions. The dimensions of such entrances and the space between the helices make more feasible binding positions parallel to the helices for long and relatively rigid molecules as ketanserin and the present ones, in agreement with the positions found in our docking experiments. The different binding modes of agonists and antagonists obtained in the present simulations could explain, at least in part, their divergent pharmacological behaviors.

In conclusion, structural modification of conformationally constrained butyrophenones generated ligands that exhibit high affinity and selectivity for the different 5-HT$_2$ receptors. Among such compounds, **11e**, **19e**, **10e**, **20g**, **13g**, and **12g** emerged as 5HT$_{2A}$ selective ligands, while **22c** turned out to be a selective 5HT$_{2C}$ ligand, and **10a** and **18a** were identified as slightly selective 5-HT$_{2B}$ ligands. These compounds may constitute interesting pharmacological tools for a deeper understanding of the role played by each 5-HT$_2$ receptor subtype in schizophrenia and other CNS disorders.

As far as the molecular modeling is concerned, the 3D-QSAR analysis allowed the identification of the main molecular determinants for a high affinity binding at the 5-HT$_{2A}$ and, to a lesser extent, at the 5-HT$_{2C}$ receptors.

Some interesting structural features, determining 5-HT$_2$ subtype selectivity, were also found. In particular, piperidine-containing derivatives showed a higher selectivity toward 5-HT$_{2A}$ and 5-HT$_{2C}$ receptors as compared to the corresponding piperazine derivatives. Some of the latter derivatives displayed some selectivity for 5-HT$_{2C}$ and, although at a lower level, for the 5-HT$_{2B}$ receptor subtype. Moreover, the highest affinity ligands at the 5-HT$_{2B}$ receptor were characterized by the presence of a two-carbon ethylene bridge between the amino and the alkanone moieties.

Finally, a docking simulation study of some ligands at 5-HT$_{2A}$ and 5-HT$_{2C}$ receptor models, provided results consistent with 3D-QSAR findings and suggested an interesting hypothesis for the antagonist binding mode.

Experimental Section

Chemistry. Melting points were determined using a Kofler hot stage instrument or a Gallenkamp capillary melting point apparatus and are uncorrected. Infrared spectra were recorded by means of a Perkin-Elmer 1600 Fourier transform infrared spectrophotometer; the main absorption bands are given in cm^{-1}. ^{1}H spectra were recorded with a Bruker WM AMX (300 MHz); chemical shifts are recorded in parts per million (δ) downfield from tetramethylsilane. Mass spectra were performed on Kratos MS-50 or Varian Mat-711 mass spectrometers in fast atom bombardment (FAB) mode (with 2-hydroxyethyl disulfide as matrix) or by electron impact (EI). Flash column chromatography was performed using Kieselgel 60 (60−200 mesh, E. Merck AG, Darmstadt, Germany). Reactions were monitored by thin-layer chromatography on Merck 60 GF$_{254}$ chromatogram sheets using iodine vapor and/or UV light for detection; unless otherwise stated, each purified compound showed a single spot. Elemental combustion analyses were performed on a Perkin-Elmer 240B apparatus at the Microanalysis Service of the Universidad de Santiago de Compostela; unless otherwise stated, all reported values are within ±0.4% of the theoretical compositions. Solvents were purified as per Vogel[97] by distillation over the drying agent under an argon atmosphere and were used immediately. Unless otherwise stated, hydrochlorides were prepared by dropwise addition, with cooling, of a saturated solution of HCl in anhydrous

ether to a solution of the amine in anhydrous ether or absolute ethanol/ether.

4-Oxo-4,5,6,7-tetrahydrobenzo[*b*]furan-5-ylacetic Acid (29). To a stirred mixture of diisopropylamine (2.98 mL, 0.021 mol) in dry tetrahydrofuran (THF, 200 mL) at −20 °C, a 2.5 M solution of *n*-BuLi in hexane (8.53 mL, 0.021 mol) was added. The mixture was stirred for 30 min at −20 °C and for another 30 min at −70 °C. After this time, a solution of 4,5,6,7-tetrahydrobenzo[*b*]furan-4-one (2.86 g, 0.021 mol) in dry THF (60 mL) was added dropwise. After the solution was stirred for 1 h at −70 °C, ethyl bromoacetate (2.0 mL, 0.021 mol) was added, and the mixture was stirred for 30 min at −70 °C and then for 18 h at room temperature. The solvent was removed in vacuo, and the residue was dissolved in AcOEt and washed with water, 5% NaHCO₃, and 5% HCl. The organic extracts were dried (Na₂SO₄) and concentrated to give a residue that was purified by column chromatography (CH₂Cl₂) to yield ethyl 4-oxo-4,5,6,7-tetrahydrobenzo[*b*]furan-5-yl acetate (3.22 g, 69%) as a pale yellow oil. To a solution of this ester (2.0 g, 9 mmol) in methanol (10 mL), a 10% solution of NaOH in methanol (10.8 mL, 27 mmol) was added. The mixture was stirred at reflux temperature for 2 h. After this time, the solvent was removed under reduced pressure; the residue was dissolved in water, washed with CH₂Cl₂, and acidified with concentrated HCl. The solid precipitate was collected by filtration and crystallized from H₂O to give the acid **29** (1.31 g, 75%) as white crystals of mp 103−104 °C. IR: 3100, 1732, 1641, 1582. ^{1}H NMR (DMSO-d_6): δ 1.97 (dq, 1H, $J = 5.7, 1.3, 1H_6$); 2.18−2.20 (m, 1H, $1H_6$); 2.34 (dd, 1H, $J = 16.5, 6.6, -H$CH−COOH); 2.66 (dd, 1H, $J = 16.5, 5.4$ Hz, −HCH−COOH); 2.74−2.93 (m, 3H, H_5, $2H_7$); 6.64 (d, 1H, $J = 2, H_3$); 7.66 (d, 1H, $J = 1.8, H_2$); 12.12 (s, 1H, −OH). MS (EI, *m/z*): 194 (M⁺). Anal. ($C_{10}H_{10}O_4$) C, H.

General Procedure for Synthesis of Ketoamides 25−27 and 30−33. A solution of the amine (10 mmol), HOBt (1.35 g, 10 mmol), and the corresponding carboxylic acid (10 mmol) in anhydrous CH₂Cl₂ (25 mL) was stirred under argon at room temperature for 15 min and then cooled to 0 °C. At this temperature, DCC (2.06 g, 10 mmol) was added and the reaction mixture was kept at 0−5 °C for 1 h and then allowed to reach room temperature and left overnight. The precipitated 1,3-dicyclohexylurea was filtered off, and the filtrate was washed several times with 5% NaHCO₃ and water, dried (Na₂SO₄), and condensed to dryness. The oily residue was purified by flash chromatography (AcOEt/hexane) to give the amide as a white crystalline solid. The synthesis of each particular amide is described below.

1-[(1-Oxo-indan-3-yl)carbonyl]-4-(2-pyridyl)piperazine (25). Compound **25** was prepared from 3-oxo-indane-1-carboxylic acid, yield 87%, mp 175−177 °C (*i*-PrOH). IR: 1714, 1644. ^{1}H NMR (CDCl₃): δ 2.87 (dd, 1H, $J = 18.5, 7.5, H_2$ indanone); 2.98 (dd, 1H, $J = 18.5, 4.1, H_2$ indanone); 3.55−3.91 (m, 8H, piperazine); 4.59 (dd, 1H, $J = 7.4, 4.2, H_3$ indanone); 6.64−6.71 (m, 2H, H_3 and H_5 pyridine); 7.28 (t, 1H, $J = 7.3, H_6$ indanone); 7.39−7.42 (m, 1H, H_4 pyridine); 7.50−7.61 (m, 2H, H_4 and H_5 indanone); 7.71 (t, 1H, $J = 8.3, H_7$ indanone); 8.16 (dd, 1H, $J = 4.9, 1.5, H_6$ pyridine). MS (FAB, *m/z*): 322 (MH⁺). Anal. ($C_{19}H_{19}N_3O_2$) C, H, N.

1-[(1-Oxoindan-2-yl)acetyl]-4-(*o*-methoxyphenyl)piperazine (26). Compound **26** was prepared from (1-oxo-2-indanyl)acetic acid, yield 85%, mp 138−139 °C (EtOH). IR: 1702, 1644, 1600. ^{1}H NMR (CDCl₃): δ 2.69 (dd, 1H, $J = 17.2, 9.2$, HCH−CONRR); 2.95 (dd, 1H, $J = 17.0, 4.2, H_3$ indanone); 3.03−3.14 (m, 2H, H_2 indanone, HCH−CONRR); 3.18−3.28 (m, 4H, −CON(CH₂−CH_2)₂N−); 3.53 (dd, 1H, $J = 17.0, 7.4, H_3$ indanone); 3.76−3.87 (m, 4H, −CON(CH_2−CH₂)₂N−); 3.91 (s, 3H, −OCH₃); 6.92−7.18 (m, 4H, Ph); 7.38 (d, 1H, $J = 7.4, H_6$ indanone); 7.47 (d, 1H, $J = 7.3, H_4$ indanone); 7.60 (dt, 1H, $J = 7.4, 1.1, H_5$ indanone); 7.78 (d, 1H, $J = 7.6, H_7$ indanone). MS (FAB, *m/z*): 365 (MH⁺). Anal. ($C_{22}H_{24}N_2O_3$) C, H, N.

1-[(4-Oxo-4,5,6,7-tetrahydrobenzo[*b*]thiophen-5-yl)acetyl]-4-(2-pyridyl)piperazine (27). Compound **27** was prepared from (4-oxo-4,5,6,7-tetrahydrobenzo[*b*]thiophen-5-yl)-acetic acid, yield 85%, mp 135−137 °C (MeOH−ether). IR:

1669, 1635, 1592. ^{1}H NMR (CDCl₃): δ 1.97−2.08 (m, 1H, H_6 benzothiophene); 2.28−2.43 (m, 1H, H_6 benzothiophene); 2.34 (dd, 1H, $J = 17.3, 7.5, H$CH−CONRR); 3.07−3.22 (m, 4H, $2H_7$ and H_5 benzothiophene, −HCH−CONRR); 3.50−3.83 (m, 8H, piperazine); 6.61−6.65 (m, 2H, H_3 and H_5 pyridine); 7.03 (d, 1H, $J = 5.2, H_2$ benzothiophene); 7.34 (d, 1H, $J = 5.2, H_3$ benzothiophene); 7.45−7.50 (m, 1H, H_4 pyridine); 8.16 (dd, 1H, $J = 4.9, 1.6, H_6$ pyridine). MS (FAB, *m/z*): 356 (MH⁺). Anal. ($C_{19}H_{21}N_3O_2S$) C, H, N.

1-[(4-Oxo-4,5,6,7-tetrahydrobenzo[*b*]furan-5-yl)acetyl]-4-(*o*-methoxyphenyl)piperazine (30). Compound **30** was prepared from (4-oxo-4,5,6,7-tetrahydrobenzo[*b*]furan-5-yl)-acetic acid using dimethylformamide (DMF) as solvent, yield 85%, mp 121−122 °C (cyclohexane). IR: 2927, 1661, 1645. ^{1}H NMR (CDCl₃): δ 1.94−2.02 (m, 1H, $1H_6$ benzofuran); 2.26−2.34 (dd, 1H, $J = 16.2, 8.3, -H$CH−CONRR); 2.40−2.47 (m, 1H, $1H_6$ benzofuran); 2.93−3.02 (m, 3H, $2H_7$ and H_5 benzofuran); 3.03−3.09 (m, 4H, −CON(CH₂−CH_2)₂N−); 3.22 (dd, 1H, $J = 16.2, 3.6, -H$CH−CONRR); 3.71−3.74 (m, 4H, −CON-(CH_2−CH₂)₂N−); 3.88 (s, 3H, −OCH₃); 6.66 (d, 1H, $J = 2, H_3$ benzofuran); 6.87−7.01 (m, 4H, Ph); 7.32 (d, 1H, $J = 1.9, H_3$ benzofuran). MS (EI, *m/z*): 368 (M⁺). Anal. ($C_{21}H_{24}N_2O_4$) C, H, N.

1-[(4-Oxo-4,5,6,7-tetrahydrobenzo[*b*]furan-5-yl)acetyl]-4-(2-pyridyl)piperazine (31). Compound **31** was prepared from (4-oxo-4,5,6,7-tetrahydrobenzo[*b*]furan-5-yl)acetic acid using DMF as solvent, yield 90%, mp 122−123 °C (cyclohexane). IR: 2920, 1678, 1623, 1595. ^{1}H NMR (CDCl₃): δ 1.91−2.05 (m, 1H, $1H_6$ benzofuran); 2.31 (dd, 1H, $J = 16.1, 7.9, -H$CH−CONRR); 2.35−2.44 (m, 1H, $1H_6$ benzofuran); 2.93−3.23 (m, 4H, H_5 and $2H_7$ benzofuran, −HCH−CONRR); 3.50−3.81 (m, 8H, piperazine); 6.66 (d, 1H, $J = 1.9, H_3$ benzofuran); 6.64−6.68 (m, 2H, H_3 and H_5 pyridine); 7.31 (d, 1H, $J = 1.9, H_2$ benzofuran); 7.47−7.53 (m, 1H, H_4 pyridine); 8.18−8.20 (m, 1H, H_6 pyridine). MS (FAB, *m/z*): 340 (MH⁺). Anal. ($C_{19}H_{21}N_3O_3$) C, H, N.

1-[(4-Oxo-4,5,6,7-tetrahydrobenzo[*b*]furan-5-yl)acetyl]-4-(*p*-fluorobenzoyl)piperidine (32). Compound **32** was prepared from (4-oxo-4,5,6,7-tetrahydrobenzo[*b*]furan-5-yl)-acetic acid using DMF as solvent, yield 80%, mp 124−125 °C (cyclohexane). IR: 2920, 1671, 1636, 1595. ^{1}H NMR (CDCl₃): δ 1.66−1.86 (m, 4H, −N(CH₂−CH_2)₂CH−); 1.89−1.98 (m, 2H, $2H_6$ benzofuran); 2.24 (dd, 1H, $J = 16.1, 8.1, -H$CH−CO−NRR); 2.29−2.44 (m, 1H, −N(HCH−CH₂)₂CH−); 2.85−3.00 (m, 3H, $2H_7$ and H_5 benzofuran); 3.09−3.26 (m, 2H, −HCH−CO−NRR, −N(HCH−CH₂)₂CH−); 3.44−3.49 (m, 1H, RRCH−CO−Ph); 4.01−4.06 (m, 1H, −N(HCH−CH₂)₂CH−); 4.54−4.61 (m, 1H, −N(HCH−CH₂)₂CH−); 6.65 (d, 1H, $J = 1.8, H_3$ benzofuran); 7.15 (t, 2H, $J = 8.5, H_3$ and H_5 Ph); 7.31 (d, 1H, $J = 1.9, H_2$ benzofuran); 7.97 (dd, 2H, $J = 8.6, 5.4, H_2$ and H_6 Ph). MS (FAB, *m/z*): 384 (MH⁺). Anal. ($C_{22}H_{22}FNO_4$) C, H, N.

1-[(4-Oxo-4,5,6,7-tetrahydrobenzo[*b*]furan-5-yl)acetyl]-4-(6-fluorobenzisoxazol-3-yl)piperidine (33). Compound **33** was prepared from (4-oxo-4,5,6,7-tetrahydrobenzo[*b*]furan-5-yl)acetic acid using DMF as solvent, yield 80%, mp 141−143 °C (cyclohexane). IR: 2921, 1670, 1641, 1517. ^{1}H NMR (CDCl₃): δ 1.93−2.16 (m, 5H, $1H_6$ benzofuran, −N(CH₂−CH_2)₂CH−); 2.32 (dd, 1H, $J = 16.1, 7.8, -H$CH−CONRR); 2.39−2.93 (m, 2H, $1H_6$ benzofuran, −N(HCH−CH₂)₂CH−); 2.94−3.38 (m, 6H, H_5, $2H_7$, −HCH−CONRR, −N(HCH−CH₂)₂CH−, −N(CH₂−CH₂)₂CH−); 4.11 (m, 1H, −N(HCH−CH₂)₂CH−); 4.60−4.73 (m, 1H, −N(HCH−CH₂)₂CH−); 6.66 (d, 1H, $J = 1.9, H_3$ benzofuran); 7.05−7.11 (m, 1H, H_5 benzisoxazole); 7.26 (dd, 1H, $J = 5.1, 2.1, H_7$ benzisoxazole); 7.31 (d, 1H, $J = 1.9, H_2$ benzofuran); 7.70 (dd, 1H, $J = 8.7, 5.1, H_4$ benzisoxazole). MS (FAB, *m/z*): 397 (MH⁺). Anal. ($C_{22}H_{21}FN_2O_4$) C, H, N.

General Procedure for Synthesis of Aminoketones 10c, 12a, 20c, 23a, 23c, 23g, and 23h. A stirred solution of the amide (8.2 mmol), ethylene glycol (45 mL, 0.82 mol), and *p*-TsOH (50 mg) in anhydrous toluene (75 mL) was refluxed in a Dean−Stark apparatus for 4 days with azeotropic distillation of water. After the solution was cooled, the toluene solution was washed several times with 10% Na₂CO₃ and water and dried (Na₂SO₄), and the solvent was removed under

reduced pressure. The resulting crude ethylene ketal was dissolved in anhydrous ether (30 mL) and added dropwise under argon to a stirred suspension of LiAlH$_4$ (1.18 g, 31 mmol) in anhydrous ether (60 mL). The reaction mixture was heated under reflux for 8 h, cooled to 0 °C in an ice-bath, and then quenched by sequential dropwise addition of H$_2$O (1.5 mL), NaOH 10% (3 mL), and H$_2$O (4 mL). The coarse precipitate formed was filtered out and thoroughly washed with ether. The combined filtrates were treated with 10% HCl and heated under reflux for 1–2 h. On cooling, the aqueous phase was made alkaline with 10% NaOH and extracted with CH$_2$Cl$_2$ three times, the combined organic extracts were dried (Na$_2$SO$_4$), and the solvent was removed in vacuo. The residue was dissolved in anhydrous ether, and ether-saturated HCl gas was cautiously added to the resulting solution. The white precipitate formed was recovered and kept overnight in a vacuum desiccator. Each particular aminoketone is described below.

1-[(1-Oxoindan-3-yl)methyl]-4-(2-pyridyl)piperazine (10c). Yield, 85%, mp 175–177 °C (AcOEt). IR: 2945, 2825, 1717. ^{1}H NMR (CDCl$_3$): δ 2.50 (dd, 1H, J = 12.4, 8.5, HCH–NRR); 2.60 (dd, 1H, J = 19.2, 3.0, H$_2$ indanone); 2.59–2.67 (m, 4H, –CH$_2$–N(CH_2CH$_2$)$_2$–N–); 2.72 (dd, 1H, J = 12.4, 6.7, –HCH–NRR); 2.85 (dd, 1H, J = 19.3, 7.5, H$_2$ indanone); 3.51–3.61 (m, 4H, –N(CH$_2$CH_2)$_2$–N–); 3.60–3.64 (m, 1H, H$_3$ indanone); 6.62–6.69 (m, 2H, H$_3$ and H$_5$ pyridine); 7.38 (t, 1H, J = 7.3, H$_6$ indanone); 7.45–7.51 (m, 1H, H$_4$ pyridine); 7.60 (t, 1H, J = 7.4, H$_5$ indanone); 7.67 (d, 1H, J = 7.6, H$_4$ indanone); 7.75 (d, 1H, J = 7.6, H$_7$ indanone); 8.19 (dd, 1H, J = 4.8, 1.5, H$_6$ pyridine). MS (FAB, m/z): 308 (MH$^+$). Anal. (C$_{19}$H$_{21}$N$_3$O) C, H, N. Hydrochloride: mp 230–232 °C (*i*-PrOH).

1-[(1-Oxoindan-2-yl)ethyl]-4-(*o*-methoxyphenyl)piperazine (12a). Yield, 70%. IR: 2938, 1715, 1608. ^{1}H NMR (CDCl$_3$): δ 1.80–1.86 (m, 1H, HCH–CH$_2$–NRR); 2.18–2.23 (m, 1H, HCH–CH$_2$–NRR); 2.61 (t, 2H, J = 7.4, –CH$_2$–NRR); 2.69–2.80 (m, 5H, H$_2$ indanone, –CH$_2$–N(CH_2–CH$_2$)$_2$N–); 2.88 (dd, 1H, J = 17.1, 4.0, H$_3$ indanone); 3.03–3.14 (m, 4H, –CH$_2$–N(CH$_2$–CH_2)$_2$N–); 3.37 (dd, 1H, J = 17.0, 8.0, H$_3$ indanone); 3.87 (s, 3H, –OCH$_3$); 6.84–7.02 (m, 4H, Ph); 7.36 (t, 1H, J = 7.4, H$_6$ indanone); 7.47 (d, 1H, J = 7.5, H$_4$ indanone); 7.58 (t, 1H, J = 7.7, H$_5$ indanone); 7.76 (d, 1H, J = 7.6, H$_7$ indanone). MS (FAB, m/z): 351 (MH$^+$). Hydrochloride: mp 215–216 °C (MeOH–ether). Anal. (C$_{22}$H$_{26}$N$_2$O$_2$·2HCl) C, H, N.

1-[2-(4-Oxo-4,5,6,7-tetrahydrobenzo[*b*]thiophen-5-yl)ethyl]-4-(2-pyridyl)piperazine (20c). Yield, 82%. IR: 2822, 1667, 1593. ^{1}H NMR (CDCl$_3$): δ 1.62–1.73 (m, 1H, –HCH–CH$_2$–N<); 1.98–2.09 (m, 1H, H$_6$ benzothiophene); 2.17–2.38 (m, 2H, H$_6$ benzothiophene, –HCH–CH$_2$–N<); 2.53 (t, 2H, J = 7.8, –CH$_2$–N<); 2.51–2.55 (m, 1H, H$_5$ benzothiophene); 2.59 (t, 4H, J = 5.1, –N(CH_2–CH$_2$)$_2$N–Ar); 2.99–3.16 (m, 2H, H$_7$ benzothiophene); 3.53 (t, 4H, J = 5.1, N(CH$_2$–CH_2)$_2$N–Ar); 6.59–6.65 (m, 2H, H$_3$ and H$_5$ pyridine); 7.05 (d, 1H, J = 5.3, H$_2$ benzothiophene); 7.37 (d, 1H, J = 5.3, H$_3$ benzothiophene); 7.43–7.49 (m, 1H, H$_4$ pyridine); 8.17 (dd, 1H, J = 4.8, 1.3, H$_6$ pyridine). MS (FAB, m/z): 342 (MH$^+$). Hydrochloride: mp 275–277 °C (MeOH–ether). Anal. (C$_{19}$H$_{23}$N$_3$OS·3HCl) C, H, N.

1-[(4-Oxo-4,5,6,7-tetrahydrobenzo[*b*]furan-5-yl)ethyl]-4-(*o*-methoxyphenyl)piperazine (23a). Yield, 89%, mp 124–125 °C (*i*-PrOH). IR: 2935, 1674, 1596. ^{1}H NMR (CDCl$_3$): δ 1.62–1.65 (m, 1H, –HCH–CH$_2$NRR); 2.01 2.22 (m, 1H, HCH–CH$_2$NRR); 2.22–2.45 (m, 2H, 2H$_6$ benzofuran); 2.47–2.61 (m, 2H; –CH_2–NRR); 2.63–2.71 (m, 4H, –N(CH_2–CH$_2$)$_2$N–); 2.88–2.93 (m, 3H, 2H$_7$ and H$_5$ benzofuran); 3.10–3.19 (m, 4H, –N(CH$_2$–CH_2)$_2$N–); 3.85 (s, 3H, –OCH$_3$); 6.65 (d, 1H, J = 2 Hz, H$_3$ benzofuran); 6.83–7.01 (m, 4H, Ph); 7.31 (d, 1H, J = 2 Hz, H$_2$ benzofuran). MS (FAB, m/z): 355 (MH$^+$). Hydrochloride: mp 223–224 °C (MeOH). Anal. (C$_{21}$H$_{26}$N$_2$O$_3$·2HCl) C, H, N.

1-[(4-Oxo-4,5,6,7-tetrahydrobenzo[*b*]furan-5-yl)ethyl]-4-(2-pyridyl)piperazine (23c). Yield, 80%, mp 72–73 °C (*i*-PrOH). IR: 2953, 2830, 1672, 1592. ^{1}H NMR (CDCl$_3$): δ 1.55–1.62 (m, 1H, –HCH–CH$_2$–NRR); 1.90–1.98 (m, 1H, H$_6$ benzofuran); 2.13–2.20 (m, 1H, –HCH–CH$_2$–NRR); 2.23–

2.28 (m, 1H, H$_6$ benzofuran); 2.43–2.51 (m, 3H, H$_5$ benzofuran, –CH_2–NRR), 2.52–2.58 (m, 4H, –N(CH_2–CH$_2$)$_2$N–); 2.81–2.93 (m, 2H, H$_7$ benzofuran); 3.49 (t, 4H, J = 5.1, –N(CH$_2$–CH_2)$_2$N–); 6.56–6.60 (m, 2H, H$_3$ and H$_5$ pyridine); 6.62 (d, 1H, J = 1.9, H$_3$ benzofuran); 7.27 (d, 1H, J = 1.8, H$_2$ benzofuran); 7.42–7.48 (m, 1H, H$_4$ pyridine); 8.16 (d, 1H, J = 8.0, H$_6$ pyridine). MS (FAB, m/z): 326 (MH$^+$). Anal. (C$_{19}$H$_{23}$N$_3$O$_2$) C, H, N. Hydrochloride: mp 197–198 °C (*i*-PrOH).

1-[(4-Oxo-4,5,6,7-tetrahydrobenzo[*b*]furan-5-yl)ethyl]-4-(*p*-fluorobenzoyl)piperidine (23g). Yield, 85%, mp 112–113 °C (*i*-PrOH). IR: 2953, 1683, 159. ^{1}H NMR (CDCl$_3$): δ 1.52–1.64 (m, 1H, –HCH–CH$_2$–NRR); 1.84–1.97 (m, 5H, –N(CH$_2$–CH_2)$_2$CH–, –HCH–CH$_2$–NRR); 1.97–2.41 (m, 4H, –N(HCH–CH$_2$)$_2$CH–, 2H$_6$ benzofuran); 2.46–2.49 (m, 3H, –CH_2–NRR, H$_5$ benzofuran); 2.89–3.01 (m, 4H, –N(HCH–CH$_2$)$_2$CH–, 2H$_7$ benzofuran); 3.14–3.20 (m, 1H, –N(HCH–CH$_2$)$_2$CH–); 6.65 (d, 1H, J = 1.9, H$_3$ benzofuran); 7.12 (t, 2H, J = 8.6, H$_3$ and H$_5$ Ph); 7.30 (d, 1H, J = 1.9, H$_2$ benzofuran); 7.93 (dd, 2H, J = 8.7, 5.6, H$_2$ and H$_6$ Ph). MS (FAB, m/z): 370 (MH$^+$). Anal. (C$_{22}$H$_{24}$FNO$_3$) C, H, N. Hydrochloride: mp 275–276 °C (*i*-PrOH). Anal. (C$_{22}$H$_{24}$FNO$_3$·HCl) C, H, N.

1-[(4-Oxo-4,5,6,7-tetrahydrobenzo[*b*]furan-5-yl)ethyl]-4-(6-fluorobenzisoxazol-3-yl)piperidine (23h). Yield, 85%, mp 124–125 °C (*i*-PrOH). IR: 2920, 1676, 1610. ^{1}H NMR (CDCl$_3$): δ 1.57–1.70 (m, 1H, –HCH–CH$_2$–NRR); 1.94–2.48 (m, 9H, –N(HCH–CH_2)$_2$CH–, –HCH–CH$_2$–NRR, 2H$_6$ benzofuran); 2.50–2.66 (m, 3H, –CH_2–NRR, H$_5$ benzofuran); 2.83–2.98 (m, 4H, 2H$_7$ benzofuran, –N(HCH–CH$_2$)$_2$CH–); 3.03–3.12 (m, 1H, –N(HCH–CH$_2$)$_2$CH–); 6.65 (d, 1H, J = 1.9, H$_3$ benzofuran); 7.04 (dt, 1H, J = 8.8, 2.1, H$_5$ benzisoxazole); 7.07–7.27 (m, 1H, H$_7$ benzisoxazole); 7.31 (d, 1H, J = 1.9, H$_2$ benzofuran); 7.69 (dd, 1H, J = 8.7, 5.0, H$_4$ benzisoxazole). MS (FAB, m/z): 383 (MH$^+$). Anal. (C$_{22}$H$_{23}$FN$_2$O$_3$) C, H, N. Hydrochloride: mp 257–258 °C (*i*-PrOH).

1-[(1-Oxo-1,2,3,4-tetrahydro-3-naphthyl)methyl]-4-(6-fluorobenzisoxazol-3-yl)piperidine (11h). A solution of 3-(*p*-toluenesulfonyloxymethyl)-1,2,3,4-tetrahydronaphthalen-1-one[85] (0.24 g, 0.7 mmol) and 4-(6-fluorobenzisoxazol-3-yl)-piperidine (0.55 g, 1.4 mmol) in 1-methyl-2-pyrrolidone (NMP, 7 mL) was stirred at 85 °C for 24 h. The solvent was evaporated under reduced pressure, and the residue was dissolved in CH$_2$Cl$_2$ and washed with water. The organic layer was dried (Na$_2$SO$_4$), filtered, and concentrated under vacuo to give an oil, which was purified by chromatography (silica gel, EtOAc/hexane 1:1) to give the amine **11h** (0.14 g, 51%) as a yellowish oil. IR: 2941, 1684, 1616. ^{1}H NMR (CDCl$_3$): δ 2.04–2.26 (m, 6H, –CH_2–N(CH$_2$–CH_2)$_2$CH–); 2.33–2.50 (m, 4H, –CH$_2$–N(CH_2–CH$_2$)$_2$CH–); 2.74–2.90 (m, 2H, H$_3$ and H$_4$ tetralone); 3.00–3.20 (m, 4H, 2H$_2$ and H$_4$ tetralone, –N(CH$_2$-CH$_2$)$_2$CH–); 7.07 (dt, 1H, J = 8.9, 2.1, H$_5$ benzisoxazole); 7.25 (dd, 1H, J = 8.7, 2.1, H$_7$ benzisoxazole); 7.29–7.34 (m, 2H, H$_5$ and H$_7$ tetralone); 7.49 (dt, 1H, J = 7.4, 1.4, H$_6$ tetralone); 7.60–7.73 (m, 1H, H$_4$ benzisoxazole); 8.03 (d, 1H, J = 7.8, H$_8$ tetralone). MS (EI, m/z): 378 (M$^+$). Hydrochloride: mp 248–250 °C (*i*-PrOH). Anal. (C$_{23}$H$_{23}$FN$_2$O$_2$·HCl·0.75H$_2$O) C, H, N.

Methyl γ-[4-(2-Pyridyl)piperazin-1-yl]-β-(2-thenyl)butyrate (28). To a solution of *N*-(2-pyridyl)piperazine (0.82 g, 5 mmol) and methyl γ-bromo-β-thenylbutyrate (1.38 g, 5 mmol) in MIK (35 mL) were added K$_2$CO$_3$ (2.5 g) and KI (0.045 g). This mixture was refluxed for 12 h. Inorganic salts were then filtered out, and the solvent was removed under reduced pressure. The resulting oil was dissolved in CH$_2$Cl$_2$, washed several times with water, and dried (Na$_2$SO$_4$). The CH$_2$Cl$_2$ was removed under reduced pressure, and the residue was purified by column chromatography (AcOEt/hexane, 1:1) to afford the desired aminomethyl ester **28** (1.7 g, 95%) as an oil. IR: 1733, 1593. ^{1}H NMR (CDCl$_3$): δ 2.21–2.36 (m, 4H, –CH_2–N(HCH–CH$_2$)$_2$N–Ar); 2.44–2.61 (m, 5H, –CH$_2$–COO, >CH–CH$_2$–N(HCH–CH$_2$)$_2$N–Ar); 2.87–2.93 (m, 2H, thiophene–CH_2–); 3.49 (t, 4H, J = 4.6, N(CH$_2$–CH_2)$_2$N–Ar); 3.64 (s, 3H, –CO$_2$-CH$_3$); 6.58–6.64 (m, 2H, H$_3$ and H$_5$ pyridine); 6.79 (d, 1H, J = 2.9, H$_3$ thiophene); 6.92 (dd, 1H, J = 5.1, 3.4, H$_4$ thiophene); 7.14 (dd, 1H, J = 5.2, 1.0, H$_5$ thiophene); 7.46 (dd, 1H, J = 8.6, 5.2, H$_4$ pyridine); 8.17 (dd, 1H, J = 4.8, 1.7, H$_6$ pyridine).

MS (EI, *m/z*): 359 (M$^+$). Hydrochloride: mp 137−139 °C (MeOH−ether). Anal. (C$_{19}$H$_{25}$N$_3$O$_2$S·3HCl) C, H, N.

1-[(4-Oxo-4,5,6,7-tetrahydrobenzo[*b*]thiophen-6-yl)-methyl]-4-(2-pyridyl)piperazine (18c). To 34 g of PPA (Fluka), stirring under argon at 90 °C, was slowly added crude methyl γ-[4-(2-pyridyl)piperazin-1-yl]-β-(2-thenyl)butyrate **28** (1 g, 2.8 mmol), after which the temperature was increased to 130 °C. After 5 h, the reaction mixture was poured into ice-water, made alkaline with 5 N NaOH, and extracted with CH$_2$-Cl$_2$. The organic phase was washed several times with water to neutral pH and dried (Na$_2$SO$_4$), and the CH$_2$Cl$_2$ was removed in vacuo to afford the amine **18c** (0.36 g, 40%) as an oil. IR: 2927, 1669, 1594. ^{1}H NMR (CDCl$_3$): δ 2.32 (dd, 1H, *J* = 16.1, 11.1, H$_5$ benzothiophene); 2.25−2.75 (m, 7H, H$_6$ benzothiophene, −C*H*$_2$−N(C*H*$_2$−CH$_2$)$_2$N−Ar); 2.74 (dd, 1H, *J* = 17.0, 5.4, H$_7$ benzothiophene); 2.75 (dd, 1H, *J* = 16.1, 15.1, H$_5$ benzothiophene); 3.28 (dd, 1H, *J* = 16.5, 3.9, H$_7$ benzothiophene); 3.53 (t, 4H, *J* = 5.1, N(CH$_2$−C*H*$_2$)$_2$N−Ar); 6.59−6.65 (m, 2H, H$_3$ and H$_5$ pyridine); 7.07 (d, 1H, *J* = 5.3, H$_2$ benzothiophene); 7.38 (d, 1H, *J* = 5.3, H$_3$ benzothiophene); 7.47 (dd, 1H, *J* = 8.6, 5.1, H$_4$ pyridine); 8.18 (dd, 1H, *J* = 4.9, 1.2, H$_6$ pyridine). MS (FAB, *m/z*): 328 (MH$^+$). Hydrochloride: mp 144−146 °C (MeOH−ether). Anal. (C$_{18}$H$_{21}$N$_3$OS·3HCl) C, H, N.

Pharmacology. Binding and functional assays were carried out for most of the compounds prepared and plotted as shown in Figures 1 and 2.

Rat 5-HT$_{2A}$ Binding Site Assays. Male 200−250 g Sprague−Dawley rats were anaesthetized with CO$_2$ and killed by decapitation. The frontal cortex, containing 5-HT$_{2A}$ receptors,[22,15] was dissected free on ice, frozen on dry ice, and stored at −70 °C until use (generally less than 1 week later). Membrane preparation procedures were carried out at 4 °C. The tissue was thawed on ice and homogenized with 10 volumes of 0.32 M sucrose in a Polytron homogenizer (Brinkmann Instruments, Westbury, NY). The homogenate was centrifuged twice at 4 °C (900g for 10 min followed by 40 000g for 30 min). The supernatant was discarded, and the pellet was resuspended in Tris-HCl buffer (pH 8.07) in a Teflon/glass homogenizer (10 strokes by hand). The homogenate was incubated at 37 °C for 15 min to remove endogenous 5-HT and centrifuged for 30 min at 40 000g. The final pellet was resuspended in Tris-HCl buffer of pH 8.07 containing 4 mM CaCl$_2$ and 0.1% ascorbic acid. Competition at [^{3}H]ketanserin binding sites was assayed in triplicate in assay mixtures consisting of 750 μL of membrane homogenate, 50 μL of [^{3}H]-ketanserin, 50 μL of either the buffer or the compound under test, 50 μL of nonspecific masking ligand solution (1 μM methysergide) when required, and buffer to a final volume of 1 mL. Mixtures were incubated for 30 min at 37 °C. The assay was terminated by rapid filtration through Whatman GF/C filter strips (presoaked in 3% polyethylenimine) in a Brandel cell harvester (Gaithersburg, MD) followed by washing with ice-cold Tris-HCl buffer (pH 6.6) to remove unbound radioligand. The radioactivity retained on filters was determined 3 h later, by liquid scintillation counting in a beta counter (Beckman, LS-6000LL).

The nonlinear curve-fitting program Kaleidagraph (Synergy Software, Reading, PA) was used to fit the equation $E = E_{max} - [E_{max} - E_{min}/(1 + (IC_{50}/C)^n)]$, where E_{max} and E_{min} are dpm at the beginning and the end of the competition experiment, respectively; IC$_{50}$ is the drug concentration required to inhibit binding by 50%; C is the concentration of the inhibitor; and n is the slope of the sigmoidal decay. Nonspecific binding was determined experimentally in the presence of unlabeled 1 μM methysergide. K_i values were calculated from the Cheng−Prusoff equation:[98] $K_i = IC_{50}/(1 + D/K_d)$, where D is the concentration and K_d is the apparent dissociation constant of the ligand.

Bovine 5-HT$_{2C}$ Binding Site Assays. Bovine choroid plexus containing 5-HT$_{2C}$ receptors[19] was dissected free on ice, frozen on dry ice, and stored at −70 °C until use (generally less than 1 week later). Membrane preparation procedures were carried out at 4 °C. The tissue was thawed on ice and

homogenized with 10 volumes of 0.32 M sucrose in a Polytron homogenizer (Brinkmann Instruments, Westbury, NY). The homogenate was centrifuged twice at 4 °C (900g for 10 min followed by 40 000g for 30 min). The supernatant was discarded, and the pellet was resuspended in Tris-HCl buffer (pH 7.5) in a Teflon/glass homogenizer (10 strokes by hand). The homogenate was incubated at 37 °C for 15 min to remove endogenous 5-HT and centrifuged for 30 min at 40 000g. The final pellet was resuspended in Tris-HCl buffer of pH 7.5. Competition at [^{3}H]mesulergine binding sites was determined by a protocol analogous to that described above for the 5-HT$_{2A}$ binding assay, using a final [^{3}H]mesulergine concentration of 2 nM, and 1 μM mianserine as nonspecific masking ligand. The mixtures were incubated for 1 h at room temperature. Membranes were harvested on Whatman GF/B filter (presoaked in 3% polyethylenimine). The radioactivity retained on filters was determined 12 h later, by liquid scintillation counting in a beta counter (Beckman, LS-6000LL). IC$_{50}$ and K_i values were calculated as for rat 5-HT$_{2A}$ binding sites.

Antagonism of Serotonin at 5-HT$_{2A}$ Receptors from Rat Aorta. Antagonism of serotonin at 5-HT$_{2A}$ receptors[22,99] was assayed using denuded thoracic aorta from male (250−350 g) Sprague−Dawley rats, anesthetized by CO$_2$, and killed by decapitation. The descending aorta was removed, cleaned, stripped of endothelium, and cut into rings 4 mm in length[79] that were then mounted under a tension of 2 g in an organ bath containing 20 mL of Krebs solution of the following composition (mM): NaCl, 119; KCl, 4.7; MgSO$_4$·7H$_2$O, 1.2; CaCl$_2$·2H$_2$O, 1.5; KH$_2$PO$_4$, 1.2; NaHCO$_3$, 25; glucose, 11. Chlorpheniramine (1 μM) was added to block the uptake of serotonin.[100,101] The bath solution was maintained at 37 °C and aerated with carbogen (95% O$_2$, 5% CO$_2$). Before the addition of drugs, the tissue strips were equilibrated for 1 h under a 2 g load. Isometric contractions were recorded during cumulative addition of serotonin using a Grass FTO3C transducer and a Grass 7D polygraph. Following the equilibration period, the rings were sensitized by the addition of 10 μM 5-HT for 8 min. Equilibration periods (60 min)[102] were then alternated with the construction of cumulative 5-HT concentration−response curves, as per Van Rossum[103] (from 30 nM to 100 μM). Two control runs giving identical curves were followed by test runs with ketanserin or the new compounds, which were added to the bath solution 20 min before the end of the preceding equilibration period. 5-HT concentration−effect curves were fitted to the following equation using the Kaleidagraph program (Synergy Software, Reading, PA): $E = E_{max}[A]^s/EC_{50} + [A]^s$; where E_{max}, $[A]$, and s represent the maximum response, agonist concentration, and curve slope, respectively. EC$_{50}$ is the concentration of agonist that produces 50% of the maximal response. Values of EC$_{50}$ are given as mean ± sem (standard error mean). Antagonist potency was measured with a one dose method[103] in terms of pA_2 (-log concentration of antagonist required to maintain a constant response when agonist concentration is doubled), using the following equation: pA_2= log((EC$_{50}'$/EC$_{50}$) − 1)/C; where EC$_{50}$ and EC$_{50}'$ are the concentrations of the agonist whose effect is 50% of the maximal effect, in the absence and in the presence of C concentration of the antagonist, respectively.

Antagonism of Serotonin at 5-HT$_{2B}$ Receptors from Rat Stomach Fundus. Antagonism of serotonin at 5-HT$_{2B}$ receptors was assayed using rat stomach fundus from male (250−300 g) Sprague−Dawley rats, anesthetized by CO$_2$ and killed by decapitation. The stomach was dissected free from the abdomen and immersed in modified Krebs solution of the following composition (mM): NaCl, 118; KCl, 4.7; MgSO$_4$·7H$_2$O, 1.2; CaCl$_2$·2H$_2$O, 2.5; KH$_2$PO$_4$, 1.18; NaHCO$_3$, 25; glucose, 11. Strips of stomach fundus were prepared by Vane's method[105] and mounted in organ baths containing 10 mL of the same Krebs solution as above, maintained at 37 °C with aeration using carbogen (95% O$_2$, 5% CO$_2$). Before the addition of drugs, the tissue strips were equilibrated for 1 h under a 1 g load. Isometric contractions were recorded during cumulative addition of serotonin using a Grass FTO3C transducer and a Grass 7D polygraph. Then, a protocol analogous to that

described above for 5-HT$_{2A}$ receptors was followed. Concentration–response curves for 5-HT were constructed as per Van Rossum[103] over the concentration range of 0.01 nM–10 μM.

Cell Culture. Chinese hamster ovary cells (CHO-FA4 cells) that stably express the cloned human 5-HT$_{2A}$ serotonin receptor were kindly provided by Dr. Kelly Berg and Dr. William P. Clarke (University of Texas Health Science Center, San Antonio, Texas). Cells were maintained in standard tissue culture plates (150 mm diameter) in Dulbecco's modified Eagle's medium (DMEM) F-12 medium (Gibco BRL, Paisley, U.K.) supplemented with 10% fetal calf serum (FCS, Gibco BRL, Paisley, U.K.), 1% L-glutamine (BIOSTAR, Alcorcón, Spain), and 300 μg/mL hygromycin (Gibco BRL, Paisley, U.K.).

HeLa cells were transfected to stably express the cloned human 5-HT$_{2C}$ serotonin receptors. Cells were maintained in standard tissue culture plates (150 mm diameter) in DMEM (BIOSTAR, Alcorcón, Spain), supplemented with 10% FCS (BIOSTAR, Alcorcón, Spain), 1% L-glutamine (BIOSTAR, Alcorcón, Spain), and 300 μg/mL geneticine (Gibco BRL, Paisley, U.K.).

Human 5-HT$_{2A}$ Receptor Binding Assays. Prior to harvesting, stably transfected cells were grown for 24 h in DMEM F-12 medium supplemented with 10% dialyzed FCS (Gibco BRL, Paisley, U.K.) to prevent regulatory effects of 5-HT, which is present in regular FCS. The culture medium was aspirated, and cells were washed twice with ice-cold phosphate-buffered saline (PBS), scraped off the culture plate in PBS, and pelleted by centrifugation at 1000*g* for 10 min at 4 °C. Cell pellets were homogenized with a Polytron homogenizer in 50 mM Tris-HCl, pH 7.5, at 4 °C. The homogenate was centrifuged at 24 000*g* for 30 min at 4 °C, and the resulting pellet was resuspended in assay buffer (50 mM Tris-HCl, pH 7.5). Competition at [^{3}H]ketanserin binding sites was assayed in duplicate in assay mixtures containing 750 μL of membrane homogenate, 50 μL of [^{3}H]ketanserin, 50 μL of either the buffer or the compound under test, 50 μL of nonspecific masking ligand solution (1 μM methysergide) when required, and buffer to a final volume of 1 mL. Mixtures were incubated for 30 min at 37 °C. The assay was terminated by rapid filtration through Whatman GF/C filter strips (presoaked in 3% polyethylenimine) in a Brandel cell harvester (Gaithersburg, MD) followed by washing with ice-cold Tris-HCl buffer (pH 6.6) to remove unbound radioligand. The radioactivity retained on filters was determined 3 h later, by liquid scintillation counting in a beta counter (Beckman, LS-6000LL). IC$_{50}$ and K_i values were calculated as for rat 5-HT$_{2A}$ binding sites.

Human 5-HT$_{2C}$ Receptor Binding Assays. Prior to harvesting, stably transfected cells were grown for 24 h in DMEM medium supplemented with 10% dialyzed FCS (Gibco BRL). Cell membranes were obtained as for the human 5-HT$_{2A}$ binding assay. Competition at [^{3}H]mesulergine binding sites was determined by a protocol analogous to that described above for the bovine 5-HT$_{2C}$ binding assay.

Drugs. 5-Hydroxytryptamine·HCl, mianserine, and methysergide and all other drugs and chemicals were reagent grade products from Sigma-R. B. I. (Alcobendas, Spain). Aqueous solutions of all drugs as their hydrochlorides were prepared daily using distilled water. All drug concentrations mentioned above are final molar concentrations. [^{3}H]Ketanserin (60.08 Ci/mmol) and [^{3}H]mesulergine (76 Ci/mmol) were obtained from DuPont NEN (Boston, MA) and Amersham (England), respectively.

Molecular Modeling. GRID-GOLPE. The ligands were built in the most extended conformations using standard bond distances and angles as defined in SYBYL 6.5.[106] The ligand geometries were then optimized by energy minimization using the parameter set included in the MOPAC (version 6.0)[107] suite of programs, with the PM3 Hamiltonian. The molecular alignment was carried out with low energy conformers, following a protocol described in a previous publication of some of the present authors[64] and taking into account the pharmacophoric model developed by Höltje for 5-HT$_{2A}$ antagonists.[108] The centroid(s) of the aromatic system(s), the oxygen atoms

of carbonyl and methoxy groups, the isoxazolyl and pyridyl nitrogens, the charged amino group, and the carbonyl of the cycloalkanone moiety were chosen as key fitting elements for ligand superposition.[64] The molecular interaction potentials were calculated with GRID using four different atom probes, namely the sp^3 carbon (C1), the charged sp^3 nitrogen (N3$^+$), the alcoholic hydroxyl (sp^3 oxygen, O1), and the hydrophobic probe (DRY) to measure steric, electrostatic, hydrogen bonding, and hydrophobic interactions, respectively. All of the GRID calculations were performed in a box with dimensions equal to 30 Å $\times$ 20 Å $\times$ 25 Å using a grid spacing of 1 Å.

The resulting probe–target interaction energies for each compound were unfolded to produce one-dimensional vector variables for each compound, which were assembled in the so-called X matrix. This matrix was pretreated by first using a cutoff of 5 kcal/mol to produce a more symmetrical distribution of energy values and then zeroing small variable values and removing variables with small standard deviation, using appropriate cutoffs. In addition, variables taking only two, three, or four values and presenting a skewed distribution were also removed. The SRD (number of seeds = 1500, critical distance = 1.0 Å, collapsing cutoff = 2.0 Å) was applied followed by three consecutive FFD variables selection runs. PLS cross-validated analyses were performed with the leave-one-out procedure. In all cases, the optimal number of component (ONC) was chosen by monitoring the changes in the fitting (r^2) and predictive (q^2) ability of the model upon addition of a new latent variable. Because in many cases models with the highest q^2 value had a relatively large number of components, the associated risk of overfitting was avoided by selecting, from a plot of q^2 vs the number of components, the ONC as the one at which the curve starts to flatten.

Docking. Models of the transmembrane α-helices bundle of both receptor subtypes (5-HT$_{2A}$ and 5-HT$_{2C}$) were built following a procedure analogous to others previously described.[109,110] First, on the basis of the transmembrane sequences taken from the Swissprot database,[111] each helix was separately built with the Biopolymer module of Insight II[112] using constant values of angles ϕ ($-44°$) and ι ($-59°$). Then, each helix was submitted to a molecular mechanics geometrical optimization using the AMBER 4.1 program.[113] Once optimized, the seven helices were packed in agreement with the electron density maps of bovine rhodopsin.[59] To place the helices in their appropriate relative rotational position, we considered their hydrophobicity profiles as well as experimental information on the relative position of particular residues, for example, the known hydrogen bond between an Asp in TMH2 and an Asn in TMH7.[60] Then, the geometry of the resulting transmembrane bundle was geometrically optimized using again the AMBER 4.1 program.

References

(1) Martin, G. R.; Humphrey, P. P. Receptors for 5-Hydroxytryptamine: Current Perspectives on Classification and Nomenclature. *Neuropharmacology* **1994**, *33*, 261–273.

(2) Roth, B. L.; Craigo, S. C.; Choudhary, M. S.; Uluer, A.; Monsma-FJ, J.; Shen, Y.; Meltzer, H. Y.; Sibley, D. R. Binding of Typical and Atypical Antipsychotic Agents to 5-Hydroxytryptamine-6 and 5-Hydroxytryptamine-7 Receptors. *J. Pharmacol. Exp. Ther.* **1994**, *268*, 1403–1410.

(3) Hoyer, D.; Clarke, D. E.; Fozard, J. R.; Hartig, P. R.; Martin, G. R.; Mylecharane, E. J.; Saxena, P. R.; Humphrey, P. P. International Union of Pharmacology Classification of Receptors for 5-Hydroxytryptamine (Serotonin). *Pharmacol. Rev.* **1994**, *46*, 157−203.

(4) Uphouse, L. Multiple Serotonin Receptors: too Many, not Enough, or Just the Right Number? *Neurosci. Biobehav. Rev.* **1997**, *21*, 679−698.

(5) Cowen, P. J. Serotonin Receptor Subtypes: Implications for Psychopharmacology. *Br. J. Psychiatry Suppl.* **1991**, 7−14.

(6) Roth, B. L.; Willins, D. L.; Kristiansen, K.; Kroeze, W. K. 5-Hydroxytryptamine2-Family Receptors (5-Hydroxytryptamine$_{2A}$, 5-Hydroxytryptamine$_{2B}$, 5-Hydroxytryptamine$_{2C}$): Where Structure Meets Function. *Pharmacol. Ther.* **1998**, *79*, 231−257.

(7) Martin, G. R. 5-Hydroxytryptamine Receptors. *The IUPHAR Compendium of Receptor Characterization and Classification*; 1998; pp 167−185.

(8) Felder, C. C.; Kanterman, R. Y.; Ma, A. L.; Axelrod, J. Serotonin Stimulates Phospholipase A$_2$ and the Release of Arachidonic Acid in Hippocampal Neurons by a Type 2 Serotonin Receptor that is Independent of Inositolphospholipid Hydrolysis. *Proc. Natl. Acad. Sci. U.S.A.* **1990**, *87*, 2187−2191.

(9) Thellung, S.; Barzizza, A.; Maura, G.; Raiteri, M. Serotonergic Inhibition of The Mossy Fibre-Granule Cell Glutamate Transmission in Rat Cerebellar Slices. *Naunyn-Schmiedebergs Arch. Pharmacol.* **1993**, *348*, 347−351.

(10) Loric, S.; Maroteaux, L.; Kellermann, O.; Launay, J. M. Functional Serotonin-2B Receptors are Expressed by a Teratocarcinoma-Derived Cell Line During Serotoninergic Differentiation. *Mol. Pharmacol.* **1995**, *47*, 458−466.

(11) Tournois, C.; Mutel, V.; Manivet, P.; Launay, J. M.; Kellermann, O. Cross-Talk Between 5-Hydroxytryptamine Receptors in a Serotonergic Cell Line. Involvement of Arachidonic Acid Metabolism. *J. Biol. Chem.* **1998**, *273*, 17498−17503.

(12) Manivet, P.; Mouillet, R. S.; Callebert, J.; Nebigil, C. G.; Maroteaux, L.; Hosoda, S.; Kellermann, O.; Launay, J. M. PDZ-Dependent Activation of Nitric-Oxide Synthases by the Serotonin 2B Receptor. *J. Biol. Chem.* **2000**, *275*, 9324−9331.

(13) Kaufman, M. J.; Hartig, P. R.; Hoffman, B. J. Serotonin 5-HT$_{2C}$ Receptor Stimulates Cyclic GMP Formation in Choroid Plexus. *J. Neurochem.* **1995**, *64*, 199−205.

(14) Pazos, A.; Cortes, R.; Palacios, J. M. Quantitative Autoradiographic Mapping of Serotonin Receptors in the Rat Brain. II. Serotonin-2 Receptors. *Brain Res.* **1985**, *346*, 231−249.

(15) Roth, B. L.; McLean, S.; Zhu, X. Z.; Chuang, D. M. Characterization of Two [³H]Ketanserin Recognition Sites in Rat Striatum. *J. Neurochem.* **1987**, *49*, 1833−1838.

(16) Willins, D. L.; Deutch, A. Y.; Roth, B. L. Serotonin 5-HT$_{2A}$ Receptors are Expressed on Pyramidal Cells and Interneurons in the Rat Cortex. *Synapse* **1997**, *27*, 79−82.

(17) Maayani, S.; Wilkinson, C. W.; Stollak, J. S. 5-Hydroxytryptamine Receptor in Rabbit Aorta: Characterization by Butyrophenone Analogues. *J. Pharmacol. Exp. Ther.* **1984**, *229*, 346−350.

(18) Ullmer, C.; Schmuck, K.; Kalkman, H. O.; Lubbert, H. Expression of Serotonin Receptor mRNAs in Blood Vessels. *FEBS Lett.* **1995**, *370*, 215−221.

(19) Pazos, A.; Hoyer, D.; Palacios, J. M. The Binding of Serotonergic Ligands to the Porcine Choroid Plexus: Characterization of a New Type of Serotonin Recognition Site. *Eur. J. Pharmacol.* **1984**, *106*, 539−546.

(20) Pazos, A.; Probst, A.; Palacios, J. M. Serotonin Receptors in the Human Brain-III. Autoradiographic Mapping of Serotonin-1 Receptors. *Neuroscience* **1987**, *21*, 97−122.

(21) (a) Molineaux, S. M.; Jessell, T. M.; Axel, R.; Julius, D. 5-HT$_{1C}$ Receptor is a Prominent Serotonin Receptor Subtype in the Central Nervous System. *Proc. Natl. Acad. Sci. U.S.A.* **1989**, *86*, 6793−6797. (b) Pompeiano, M.; Palacios, J. M.; Mengod, G. Distribution of the serotonin 5-HT$_2$ receptor family mRNAs: comparison between 5-HT$_{2A}$ and 5-HT$_{2C}$ receptors. *Brain Res. Mol. Brain Res.* **1994**, *23*, 163−178.

(22) (a) Bradley, P. B.; Engel, G.; Feniuk, W.; Fozard, J. R.; Humphrey, P. P.; Middlemiss, D. N.; Mylecharane, E. J.; Richardson, B. P.; Saxena, P. R. Proposals for the Classification and Nomenclature of Functional Receptors for 5-Hydroxytryptamine. *Neuropharmacology* **1986**, *25*, 563−576. (b) Mengod, G.; Pompeiano, M.; Martinez-Mir, M. I.; Palacios, J. M. Localization of the mRNA for the 5-HT$_2$ receptor by in situ hybridization histochemistry. Correlation with the distribution of receptor sites. *Brain Res.* **1990**, *524*, 139−143. (c) Lopez-Gimenez, J. F.; Mengod, G.; Palacios, J. M.; Vilaro, M. T. Selective visualization of rat brain 5-HT2A receptors by autoradiography with [³H]MDL 100, 907. *Naunyn-Schmiedebergs Arch. Pharmacol.* **1997**, *356*, 446−454.

(23) Kursar, J. D.; Nelson, D. L.; Wainscott, D. B.; Cohen, M. L.; Baez, M. Molecular Cloning, Functional Expression, and Pharmacological Characterization of a Novel Serotonin Receptor (5-Hydroxytryptamine$_{2F}$) from Rat Stomach Fundus. *Mol. Pharmacol.* **1992**, *42*, 549−557.

(24) Cohen, M. L.; Fludzinski, L. A. Contractile Serotonergic Receptor in Rat Stomach Fundus. *J. Pharmacol. Exp. Ther.* **1987**, *243*, 264−269.

(25) Foguet, M.; Hoyer, D.; Pardo, L. A.; Parekh, A.; Kluxen, F. W.; Kalkman, H. O.; Stuhmer, W.; Lubbert, H. Cloning and Functional Characterization of the Rat Stomach Fundus Serotonin Receptor. *EMBO J.* **1992**, *11*, 3481−3487.

(26) Baxter, G.; Kennett, G.; Blaney, F.; Blackburn, T. 5-HT$_2$ Receptor Subtypes: a Family Re−United? *Trends Pharmacol. Sci.* **1995**, *16*, 105−110.

(27) Schmuck, K.; Ullmer, C.; Engels, P.; Lubbert, H. Cloning and Functional Characterization of the Human 5-HT$_{2B}$ Serotonin Receptor. *FEBS Lett.* **1994**, *342*, 85−90.

(28) Bonhaus, D. W.; Bach, C.; DeSouza, A.; Salazar, F. H.; Matsuoka, B. D.; Zuppan, P.; Chan, H. W.; Eglen, R. M. The Pharmacology and Distribution of Human 5-Hydroxytryptamine$_{2B}$ (5-HT$_{2B}$) Receptor Gene Products: Comparison with 5-HT2A and 5-HT2C Receptors. *Br. J. Pharmacol.* **1995**, *115*, 622−628.

(29) Kursar, J. D.; Nelson, D. L.; Wainscott, D. B.; Baez, M. Molecular Cloning, Functional Expression, and mRNA Tissue Distribution of the Human 5-Hydroxytryptamine$_{2B}$ Receptor. *Mol. Pharmacol.* **1994**, *46*, 227−234.

(30) Duxon, M. S.; Flanigan, T. P.; Reavley, A. C.; Baxter, G. S.; Blackburn, T. P.; Fone, K. C. Evidence for Expression of the 5-Hydroxytryptamine-2B Receptor Protein in the Rat Central Nervous System. *Neuroscience* **1997**, *76*, 323−329.

(31) Meltzer, H. Y. An Overview of the Mechanism of Action of Clozapine. *J. Clin. Psychiatry* **1994**, *55* (Suppl. B), 47−52.

(32) Wainscott, D. B.; Lucaites, V. L.; Kursar, J. D.; Baez, M.; Nelson, D. L. Pharmacologic Characterization of the Human 5-Hydroxytryptamine$_{2B}$ Receptor: Evidence for Species Differences. *J. Pharmacol. Exp. Ther.* **1996**, *276*, 720−727.

(33) Barker, E. L.; Westphal, R. S.; Schmidt, D.; Sanders, B. E. Constitutively Active 5-Hydroxytryptamine$_{2C}$ Receptors Reveal Novel Inverse Agonist Activity of Receptor Ligands. *J. Biol. Chem.* **1994**, *269*, 11687−11690.

(34) Ward, R. P.; Hamblin, M. W.; Lachowicz, J. E.; Hoffman, B. J.; Sibley, D. R.; Dorsa, D. M. Localization of Serotonin Subtype 6 Receptor Messenger RNA In The Rat Brain by In Situ Hybridization Histochemistry. *Neuroscience* **1995**, *64*, 1105−1111.

(35) Monsma-FJ, J.; Shen, Y.; Ward, R. P.; Hamblin, M. W.; Sibley, D. R. Cloning and Expression of a Novel Serotonin Receptor with High Affinity for Tricyclic Psychotropic Drugs. *Mol. Pharmacol.* **1993**, *43*, 320−327.

(36) Blake, T. J.; Tillery, C. E.; Reynolds, G. P. Antipsychotic Drug Affinities at alpha$_2$-Adrenoceptor Subtypes in Post-Mortem Human Brain. *J. Psychopharmacol.* (*London*) **1998**, *12*, 151−154.

(37) Bymaster, F. P.; Nelson, D. L.; DeLapp, N. W.; Falcone, J. F.; Eckols, K.; Truex, L. L.; Foreman, M. M.; Lucaites, V. L.; Calligaro, D. O. Antagonism by Olanzapine of Dopamine D$_1$, Serotonin$_{(2)}$, Muscarinic, Histamine H-$_1$ and alpha$_{(1)}$-Adrenergic Receptors In Vitro. *Schizophr. Res.* **1999**, *37*, 107−122.

(38) Michal, P.; Lysíková, M.; El-Fakahany, E. E.; Tucek, S. Clozapine interaction with the M$_2$ and M$_4$ subtypes of Muscarinic Receptors. *Eur. J. Pharmacol.* **1999**, *376*, 119−125.

(39) Seeman, P.; Corbett, R.; Van-Tol, H. H. Atypical Neuroleptics have Low Affinity for Dopamine D$_2$ Receptors or are Selective for D$_4$ Receptors. *Neuropsychopharmacology* **1997**, *16*, 93−110.

(40) Creese, I.; Burt, D. R.; Snyder, S. H. Dopamine Receptor Binding Predicts Clinical and Pharmacological Potencies of Antischizophrenic Drugs. *Science* **1976**, *192*, 481−483.

(41) Seeman, P.; Van-Tol, H. H. Dopamine Receptor Pharmacology. *Trends Pharmacol. Sci.* **1994**, *15*, 264−270.

(42) Horacek, J. Novel Antipsychotics and Extrapyramidal Side Effects. Theory and Reality. *Pharmacopsychiatry* **2000**, *33* (Suppl.), 134−142.

(43) Aghajanian, G. K.; Marek, G. J. Serotonin Model of Schizophrenia: Emerging Role of Glutamate Mechanisms. *Brain Res. Rev.* **2000**, *31*, 302−312.

(44) Green, M. F.; Marshall-BD, J.; Wirshing, W. C.; Ames, D.; Marder, S. R.; McGurk, S.; Kern, R. S.; Mintz, J. Does Risperidone Improve Verbal Working Memory in Treatment-Resistant Schizophrenia? *Am. J. Psychiatry* **1997**, *154*, 799−804.

(45) Sipes, T. E.; Geyer, M. A. DOI Disrupts Prepulse Inhibition of Startle in Rats Via 5-HT$_{2A}$ Receptors in the Ventral Pallidum. *Brain Res.* **1997**, *761*, 97−104.

(46) Gleason, S. D.; Shannon, H. E. Blockade of Phencyclidine-Induced Hyperlocomotion by Olanzapine, Clozapine and Serotonin Receptor Subtype Selective Antagonists in Mice. *Psychopharmacology* **1997**, *129*, 79−84.

(47) Okuyama, S.; Chaki, S.; Kawashima, N.; Suzuki, Y.; Ogawa, S.; Kumagai, T.; Nakazato, A.; Nagamine, M.; Kamaguchi, K.; Tomisawa, K. The Atypical Antipsychotic Profile of NRA0045, a Novel Dopamine D4 and 5-Hydroxytryptamine₂A Receptor Antagonist, in Rats. *Br. J. Pharmacol.* **1997**, *121*, 515−525.

(48) Ereshefsky, L.; Riesenman, C.; True, J. E.; Javors, M. Serotonin-Mediated Increase in Cytosolic [Ca++] in Platelets of Risperidone-Treated Schizophrenia Patients. *Psychopharmacol. Bull.* **1996**, *32*, 101−106.

(49) Schmidt, C. J. *Development of a Selective 5-HT₂A Receptor Antagonist for the Treatment of Schizophrenia*. Presented at IBS's International Conference on Serotonin Receptors. Targets for New Therapeutic Agents, 1996.

(50) Padich, R. A.; McCloskey, T. C.; Kehne, J. H. 5-HT Modulation of Auditory and Visual Sensorimotor Gating: II. Effects of the 5-HT₂A Antagonist MDL 100, 907 on Disruption of Sound and Light Prepulse Inhibition Produced by 5-HT Agonists in Wistar Rats. *Psychopharmacology* **1996**, *124*, 107−116.

(51) Martin, P.; Waters, N.; Carlsson, A.; Carlsson, M. L. The Apparent Antipsychotic Action of the 5-HT₂A Receptor Antagonist M100907 in a Mouse Model of Schizophrenia is Counteracted by Ritanserin. *J. Neural Transm.* **1997**, *104*, 561−564.

(52) Herrick-Davis, K.; Grinde, E.; Teitler, M. Inverse agonist activity of atypical antipsychotic drugs at human 5-hydroxytryptamine₂C receptors. *J. Pharmacol. Exp. Ther.* **2000**, *295*, 226−232.

(53) Meltzer, H. Y.; McGurk, S. R. The Effects of Clozapine, Risperidone, and Olanzapine on Cognitive Function in Schizophrenia. *Schizophr. Bull.* **1999**, *25*, 233−255.

(54) Reavill, C.; Kettle, A.; Holland, V.; Riley, G.; Blackburn, T. P. Attenuation of Haloperidol-Induced Catalepsy by a 5-HT₂C Receptor Antagonist. *Br. J. Pharmacol.* **1999**, *126*, 572−574.

(55) Knable, M. B.; Weinberger, D. R. Dopamine, the Prefrontal Cortex and Schizophrenia. *J. Psychopharmacol.* **1997**, *11*, 123−131.

(56) Cussac, D.; Newman, T. A.; Nicolas, J. P.; Boutin, J. A.; Millan, M. J. Antagonist Properties of the Novel Antipsychotic, S16924, at Cloned, Human Serotonin 5-HT₂C Receptors: a Parallel Phosphatidylinositol and Calcium Accumulation Comparison with Clozapine and Haloperidol. *Naunyn-Schmiedebergs Arch. Pharmacol.* **2000**, *361*, 549−554.

(57) Palczewski, K.; Kumasaka, T.; Hori, T.; Behnke, C. A.; Motoshima, H.; Fox, B. A.; Le Trong, I.; Teller, D. C.; Okada, T.; Stenkamp, R. E.; Yamamoto, M.; Miyano, M. Crystal Structure of Rhodopsin: a G Protein-Coupled Receptor. *Science* **2000**, *289*, 739−745.

(58) Wang, C. D.; Gallaher, T. K.; Shih, J. C. Site-Directed Mutagenesis of the Serotonin 5-Hydroxytryptamine₂ Receptor: Identification of Amino Acids Necessary for Ligand Binding and Receptor Activation. *Mol. Pharmacol.* **1993**, *43*, 931−940.

(59) Baldwin, J. M.; Schertler, G. F.; Unger, V. M. An Alpha-carbon Template for the transmembrane Helices in the Rhodopsin Family of G-Protein-Coupled Receptors. *J. Mol. Biol.* **1997**, *272*, 144−164.

(60) Sealfon, S. C.; Chi, L.; Ebersole, B. J.; Rodic, V.; Zhang, D.; Ballesteros, J. A.; Weinstein, H. Related Contribution of Specific Helix 2 And 7 Residues to Conformational Activation of the Serotonin 5-HT₂A Receptor. *J. Biol. Chem.* **1995**, *270*, 16683−16688.

(61) Almaula, N.; Ebersole, B. J.; Zhang, D.; Weinstein, H.; Sealfon, S. C. Mapping The Binding Site Pocket of the Serotonin 5-Hydroxytryptamine₂A Receptor. Ser3.36(159) Provides a Second Interaction Site for the Protonated Amine of Serotonin but not of Lysergic Acid Diethylamide or Bufotenin. *J. Biol. Chem.* **1996**, *271*, 14672−14675.

(62) Kristiansen, K.; Dahl, S. G.; Edvardsen, Ø. A Database of Mutants and Effects of Site-Directed Mutagenesis Experiments on G-Protein Coupled Receptors. *Proteins: Struct., Funct., Genet.* **1996**, *26*, 81−94.

(63) Kristiansen, K.; Kroeze, W. K.; Willins, D. L.; Gelber, E. I.; Savage, J. E.; Glennon, R. A.; Roth, B. L. A Highly Conserved Aspartic Acid (Asp-155) Anchors the Terminal Amine Moiety of Tryptamines and Is Involved in Membrane Targeting of the 5-HT₂A Serotonin Receptor but does not Participate in Activation via a "Salt-Bridge Disruption" Mechanism. *J. Pharmacol. Exp. Ther.* **2000**, *293*, 735−746.

(64) Raviña, E.; Negreira, J.; Cid, J.; Masaguer, C. F.; Rosa, E.; Rivas, M. E.; Fontenla, J. A.; Loza, M. I.; Tristan, H.; Cadavid, M. I.; Sanz, F.; Lozoya, E.; Carotti, A.; Carrieri, A.; Conformationally Constrained Butyrophenones with Mixed Dopaminergic (D₂) and Serotoninergic (5-HT2A, 5-HT2C) Affinities: Synthesis, Pharmacology, 3D-QSAR, and Molecular Modeling of (Aminoalkyl)-benzo- and -thienocycloalkanones as Putative Atypical Antipsychotics. *J. Med. Chem.* **1999**, *42*, 2774−2797.

(65) Konvicka, K.; Guarnieri, F.; Ballesteros, J. A.; Weinstein, H. A proposed Structure for Transmembrane Segment 7 of G Protein Coupled Receptors Incorporating an Asn-Pro/Asp-Pro Motif. *Biophys. J.* **1998**, *75*, 601−611.

(66) Forbes, I. T.; Dabbs, S.; Duckworth, D. M.; Ham, P.; Jones, G. E.; King, F. D.; Saunders, D. V.; Blaney, F. E.; Naylor, C. B.; Baxter, G. S.; Blackburn, T. P.; Kennett, G. A.; Wood, M. D. Synthesis, Biological Activity, and Molecular Modeling of Selective 5-HT(2C/2B) Receptor Antagonists. *J. Med. Chem.* **1996**, *39*, 4966−4977.

(67) Kennett, G. A.; Wood, M. D.; Bright, F.; Cilia, J.; Piper, D. C.; Gager, T.; Thomas, D.; Baxter, G. S.; Forbes, I. T.; Ham, P.; Blackburn, T. P. In Vitro And In Vivo Profile of SB 206553, a Potent 5-HT2C/5-HT2B Receptor Antagonist with Anxiolytic-Like Properties. *Br. J. Pharmacol.* **1996**, *117*, 427−434.

(68) Bromidge, S. M.; Dabbs, S.; Davies, D. T.; Duckworth, D. M.; Forbes, I. T.; Ham, P.; Jones, G. E.; King, F. D.; Saunders, D. V.; Starr, S.; Thewlis, K. M.; Wyman, P. A.; Blaney, F. E.; Naylor, C. B.; Bailey, F.; Blackburn, T. P.; Holland, V.; Kennett, G. A.; Riley, G. J.; Wood, M. D. Novel and selective 5-HT2C/2B receptor antagonists as potential anxiolytic agents: Synthesis, quantitative structure−activity relationships, and molecular modeling of substituted 1-(3-pyridylcarbamoyl)indolines. *J. Med. Chem.* **1998**, *41*, 1598−1612.

(69) Bromidge, S. M.; Dabbs, S.; Davies, D. T.; Davies, S.; Duckworth, D. M.; Forbes, I. T.; Gaster, L. M.; Ham, P.; Jones, G. E.; King, F. D.; Mulholland, K. R.; Saunders, D. V.; Wyman, P. A.; Blaney, F. E.; Clarke, S. E.; Blackburn, T. P.; Holland, V.; Kennett, G. A.; Lightowler, S.; Middlemiss, D. N.; Trail, B.; Riley, G. J.; Wood, M. D. Biarylcarbamoylindolines are Novel and Selective 5-HT2C Receptor Inverse Agonists: Identification of 5-Methyl-1-[[2-[(2-Methyl-3-Pyridyl)Oxy]-5-Pyridyl]Carbamoyl]-6-Trifluoromethylindoline (SB-243213) as a Potential Antidepressant/Anxiolytic Agent. *J. Med. Chem.* **2000**, *43*, 1123−1134.

(70) Weinhardt, K. K.; Bonhaus, D. W.; De Souza, A. Some Benzenesulfonamido-Substituted Valerophenones that are Selective Antagonists for the 5-HT2C Receptor. *Bioorg. Med. Chem. Lett.* **1996**, *6*, 2692.

(71) Bonhaus, D. W.; Flippin, L. A.; Greenhouse, R. J.; Jaime, S.; Rocha, C.; Dawson, M.; Van Natta, K.; Chang, L. K.; Pulido-Rios, T.; Webber, A.; Leung, E.; Eglen, R. M.; Martin, G. R. RS-127445: a Selective, High Affinity, Orally Bioavailable 5-HT2B Receptor Antagonist. *Br. J. Pharmacol.* **1999**, *127*, 1075−1082.

(72) Nozulak, J.; Kalkman, H. O.; Floersheim, P.; Hoyer, D.; Schoeffter, P.; Buerki, H. R. (+)-*cis*-4,5,7a,8,9,10,11,11a-octahydro-7H-10-methylindolo[1,7-bc] [2,6]naphthyridine: a 5-HT2C/2B Receptor Antagonist with Low 5-HT2A Receptor Affinity. *J. Med. Chem.* **1995**, *38*, 28−33.

(73) Bös, M.; Stadler, H.; Wichmann, J.; Jenck, F.; Martin, J. R.; Moreau, J. L.; Sleight, A. J. Synthesis of O-methylasparvenone-derived Serotonin-Receptor Antagonists. *Helv. Chim. Acta* **1998**, *91*, 525−538.

(74) Claudi, F.; Scoccia, L.; Giorgioni, G.; Accorroni, B.; Marucci, G.; Gessi, S.; Siniscalchi, A.; Borea, P. A. 4-(4-fluorobenzoyl)-1-[2-(4-iodo-2,5-dimethoxyphenyl)ethyl]piperidine and its Derivatives: Synthesis and Affinity at 5-HT2A, 5-HT2B and 5-HT2C Serotonin Receptors. *Eur. J. Med. Chem.* **1999**, *34*, 843−852.

(75) Forbes, I. T.; Ham, P.; Booth, D. H.; Martin, R. T.; Thompson, M.; Baxter, G. S.; Blackburn, T. P.; Glen, A.; Kennett, G. A.; Wood, M. D. 5-Methyl-1-(3-pyridylcarbamoyl)-1,2,3,5-tetrahydropyrrolo[2,3-f]indole: a Novel 5-HT2C/5-HT2B Receptor Antagonist with Improved Affinity, Selectivity, and Oral Activity. *J. Med. Chem.* **1995**, *38*, 2524−2530.

(76) Cortizo, L.; Santana, L.; Raviña, E.; Orallo, F.; Fontenla, J. A.; Castro, E.; Calleja, J. M.; de Ceballos, M. L. Synthesis and Antidopaminergic Activity of Some 3-(aminomethyl)tetralones as Analogues of Butyrophenone. *J. Med. Chem.* **1991**, *34*, 2242−2247.

(77) Fontenla, J. A.; Osuna, J.; Rosa, E.; Castro, M. E.; Ferreiro, T.; Loza, M. I.; Calleja, J. M.; Sanz, F.; Rodriguez, J.; Raviña, E.; Fueyo, J.; Masaguer, C. F.; Vidal, A.; de Ceballos, M. L. Synthesis and Atypical Antipsychotic Profile of some 2-(2-piperidinoethyl)benzocycloalkanones as Analogues of Butyrophenone. *J. Med. Chem.* **1994**, *37*, 2564−2573.

(78) Loza, M. I.; Verde, I.; Castro, M. E.; Orallo, F.; Fontenla, J. A.; Calleja, J. M.; Raviña, E.; Cortizo, L.; de Ceballos, M. L. 5-HT₂ Antagonist Activity of 2-Aminomethyltetralones. *Bioorg. Med. Chem. Lett.* **1991**, *1*, 717−720.

(79) Loza, M. I.; Ferreiro, T. G.; Sanz, F.; Lozoya, E.; Rodriguez, J.; Manaut, F.; Verde, I.; Castro, E.; Fontenla, J. A.; Cadavid, I.; Honrubia, A.; Fueyo, J.; Raviña, E. Antiserotoninergic Activity of 2-aminoethylbenzocyclanones in Rat Aorta: Structure−Activity Relationships. *J. Pharm. Sci.* **1993**, *82*, 513−517.

(80) Raviña, E.; Fueyo, J.; Masaguer, C. F.; Negreira, J.; Cid, J.; Loza, I.; Honrubia, A.; Tristan, H.; Ferreiro, T.; Fontenla, J. A.; Rosa, E.; Calleja, J. M.; de Ceballos, M. L. Synthesis And Affinities For Dopamine (D₂) and 5-Hydroxytryptamine (5-HT₂A) Receptors of 1-(benzoylpropyl)-4-(1-oxocycloalkyl-2-ethyl)-piperazines as Cyclic Butyrophenone Derivatives. *Chem. Pharm. Bull.* **1996**, *44*, 534−541.

(81) Masaguer, C. F.; Raviña, E.; Fontenla, J. A.; Brea, J.; Tristan, H.; Loza, M. I. Butyrophenone Analogues in the Carbazole Series as Potential Atypical Antipsychotics: Synthesis and Determination of Affinities at D2, 5-HT2A, 5-HT2B and 5-HT2C Receptors. *Eur. J. Med. Chem.* **2000**, *35*, 83−95.

(82) Masaguer, C. F.; Casariego, I.; Raviña, E. Conformationally Restricted Butyrophenones with Mixed Dopaminergic (D2) and Serotoninergic (5-HT2A) affinities. Synthesis of 5-aminoethyl- and 6-aminomethyl-4-oxotetrahydroindoles as Potential Atypical Antipsychotics. *Chem. Pharm. Bull.* **1999**, *47*, 621−632.

(83) Masaguer, C. F.; Formoso, E.; Raviña, E.; Tristan, H.; Loza, M. I.; Rivas, E.; Fontenla, J. A. Butyrophenone Analogues in the Carbazole Series: Synthesis and Determination of Affinities at D2 and 5-HT2A Receptors. *Bioorg. Med. Chem. Lett.* **1998**, *8*, 3571−3576.

(84) Ravina, E.; Casariego, I.; Masaguer, C. F.; Fontenla, J. A.; Montenegro, G. Y.; Rivas, M. E.; Loza, M. I.; Enguix, M. J.; Villazon, M.; Cadavid, M. I.; Demontis, G. C. Conformationally Constrained Butyrophenones with Affinity for Dopamine (D1, D2, D4) and Serotonin (5-HT2A, 5-HT2B, 5-HT2C) Receptors. Synthesis of aminomethylbenzoy[*b*]furanones, and their Evaluation as Antipsychotics. *J. Med. Chem.* **2000**, *43*, 4678−4693.

(85) Julia, S.; Bonnet, Y. Etude des cétones avec noyau cyclopropane I. Les benzo- et naphtho- bicyclo- (0,1,4) hepténones. *B. Soc. Chim. Fr.* **1957**, 1340−1347.

(86) Cramer, R. D.; Patterson, D.; Bunce, J. D. Comparative Molecular Field Analysis (COMFA). 1. Effects of Shape on Binding of Steroids to Carrier Protein. *J. Am. Chem. Soc.* **1988**, *110*, 5959−5967.

(87) Baroni, M.; Constantino, G.; Cruciani, G.; Valigi, R.; Clementi, S. Generating Optimal Linear PLS Estimation (GOLPE): An Advanced Chemometric Tool for Handling 3D QSAR Problems. *Quant. Struct.-Act. Relat.* **1993**, *12*, 9−20.

(88) Dunn, W. J., III; Wold, S.; Edlund, U.; Hellberg, S.; Gasteiger, J. Multivariate Structure−Activity Relationships Between Data from a Battery of Biological Tests and an Ensemble of Chemical Descriptors: The PLS Methodol. *Quant. Struct.-Act. Relat.* **1984**, *3*, 131−137.

(89) Goodford, P. J. A Computational Procedure for Determining Energetically Favorable Binding Sites on Biologically Important Macromolecules. *J. Med. Chem.* **1985**, *28*, 849−857.

(90) Pastor, M.; Cruciani, G.; Clementi, S. Smart Region Definition: a New Way to Improve the Predictive Ability and Interpretability of Three-Dimensional Quantitative Structure−Activity Relationships. *J. Med. Chem.* **1997**, *40*, 1455−1464.

(91) Gaillard, P.; Carrupt, P. A.; Testa, B.; Boudon, A. Molecular Lipophilicity Pontential, a Tool in 3D QSAR: Method and Applications. *J. Comput.-Aided Mol. Des.* **1994**, *8*, 83−96.

(92) Laskowski, R. A.; MacArthur, M. W.; Moss, D. S.; Thornton, J. M. PROCHECK: a Program to Check the Stereochemical Quality of Protein Structures. *J. Appl. Crystallogr.* **1993**, *26*, 283−291.

(93) McMartin, C.; Bohacek, R. S. QXP: Powerful Rapid Computer Algorithms for Structure-Based Drug Design. *J. Comput.-Aided Mol. Des.* **1997**, *11*, 333−344.

(94) Johnson, M. P.; Wainscott, D. B.; Lucaites, V. L.; Baez, M.; Nelson, D. L. Mutations of Transmembrane IV and V Serines Indicate that all Tryptamines do not Bind to the Rat 5-HT2A Receptor in the Same Manner. *Mol. Brain Res.* **1997**, *49*, 1−6.

(95) Wang, C. D.; Gallaher, T. K.; Shih, J. C. Site-Directed Mutagenesis of the Serotonin 5-Hydroxytryptamine2 Receptor: Identification of Amino Acids Necessary for Ligand Binding and Receptor Activation. *Mol. Pharmacol.* **1993**, *43*, 931−940.

(96) Almaula, N.; Ebersole, B. J.; Ballesteros, J. A.; Weinstein, H.; Sealfon, S. C. Contribution of a Helix 5 Locus to Selectivity of Hallucinogenic and Nonhallucinogenic Ligands for the Human 5-Hydroxytryptamine2A and 5-Hydroxytryptamine2C Receptors: Direct and Indirect Effects on Ligand Affinity Mediated by the Same Locus. *Mol. Pharmacol.* **1996**, *50*, 34−42.

(97) Vogel, A. I. *Vogel's Textbook of Practical Organic Chemistry*, 5th ed.; Longman: Harlow, U.K., 1989.

(98) Cheng, Y.; Prusoff, W. H. Relationship Between the Inhibition Constant (K1) and the Concentration of Inhibitor which Causes 50 Per Cent Inhibition (I50) of an Enzymatic Reaction. *Biochem. Pharmacol.* **1973**, *22*, 3099−3108.

(99) Hoyer, D.; Martin, G. R. Classification and Nomenclature of 5-HT Receptors: A Comment on Current Issues. *Behav. Brain Res.* **1996**, *73*, 263−268.

(100) Gruetter, C. A.; Lemke, S. M.; Anestis, D. K.; Szarek, J. L.; Valentovic, M. A. Potentiation of 5-Hydroxytryptamine-Induced Contraction in Rat Aorta by Chlorpheniramine, Citalopram and Fluoxetine. *Eur. J. Pharmacol.* **1992**, *217*, 109−118.

(101) Fukuda, S.; Su, C.; Lee, T. J. Mechanisms of Extraneuronal Serotonin Uptake in the Rat Aorta. *J. Pharmacol. Exp. Ther.* **1986**, *239*, 264−269.

(102) Cohen, M. L.; Fuller, R. W.; Wiley, K. S. Evidence for 5-HT2 Receptors Mediating Contraction in Vascular Smooth Muscle. *J. Pharmacol. Exp. Ther.* **1981**, *218*, 421−425.

(103) Van Rossum, J. M. Cumulative dose−response curves II. Technique for the making of dose−response curves in the isolated organs and the evaluation of drug parameters. *Arch. Intern. Med.* **1963**, 143−299.

(104) MacKay, D. How Should Values of pA2 and Affinity Constants for Pharmacological Competitive Antagonists be Estimated? *J. Pharm. Pharmacol.* **1978**, *30*, 312−313.

(105) Vane, J. R. A sensitive method for the assay of 5-hydroxytryptamine. *Br. J. Pharmacol.* **1957**, *12*, 344−349.

(106) SYBYL 6.5. Tripos Association, St. Louis, MO.

(107) Stewart, J. J. P. MOPAC: a semiempirical orbital program. *J. Comput.-Aided Mol. Des.* **1990**, *4*, 1−103.

(108) Holtje, H. D.; Folkers, G. *Molecular Modeling: Basic Principles and Applications*; VCH: Weinheim, 1997.

(109) Ballesteros, J. A.; Weinstein, H. Integrated Methods for the Construction of Three-Dimensional Models and Computacional Probing of Structure−Function Relations in G Protein Coupled Receptors. *Methods Neurosci.* **1995**, *25*, 366−428.

(110) Carrieri, A.; Centeno, N. B.; Rodrigo, J.; Sanz, F.; Carotti, A. Theoretical evidence of a salt bridge disruption as the initiating process for the α1d-adrenergic receptor activation: a molecular dynamics and docking study. *Proteins* **2001**, *43*, 382−394.

(111) Attwood, T. K.; Beck, M. E.; Flower, D. R.; Scordis, P.; Selley, J. N. The PRINTS Protein Fingerprint Database in its Fifth Year. *Nucleic Acids Res.* **1998**, *26*, 304−308.

(112) Insight II, 98.0. Molecular Simulation Inc.: San Diego, 1998.

(113) Pearlman, D. A.; Case, D. A.; Caldwell, J. W.; Ross, W. S.; Cheatham, T. E., III; Ferguson, D. M.; Seibel, G. L.; Singh, U. C.; Weiner, P. K.; Kollman, P. A. AMBER, version 4.1; 1995.

JM011014Y